Supporting Information

Driving and photo-regulation of myosin-actin motor at molecular and macroscopic level by photo-responsive high energy molecules.

Halley M. Menezes,[1,2] Md. Jahirul Islam,[1,2] Masayuki Takahashi[3] and Nobuyuki Tamaoki[1,2]*

[1]Research Institute for Electronic Science, Hokkaido University, Kita 20, Nishi 10, Kita-Ku, Sapporo, Hokkaido, 001-0020, Japan.

[2]Graduate School of Life Science, Hokkaido University, Kita 10, Nishi 8, Kita-ku, Sapporo, Hokkaido, 060-0810, Japan.

[3]Faculty of Science, Hokkaido University, Kita 13, Nishi 8, Kita-Ku, Sapporo, Hokkaido, 060-0810, Japan.

E-mail: *tamaoki@es.hokudai.ac.jp*

Table of contents

1. Synthetic schemes of AzoTP derivatives.

Scheme of AzoethoxyTP (4b)

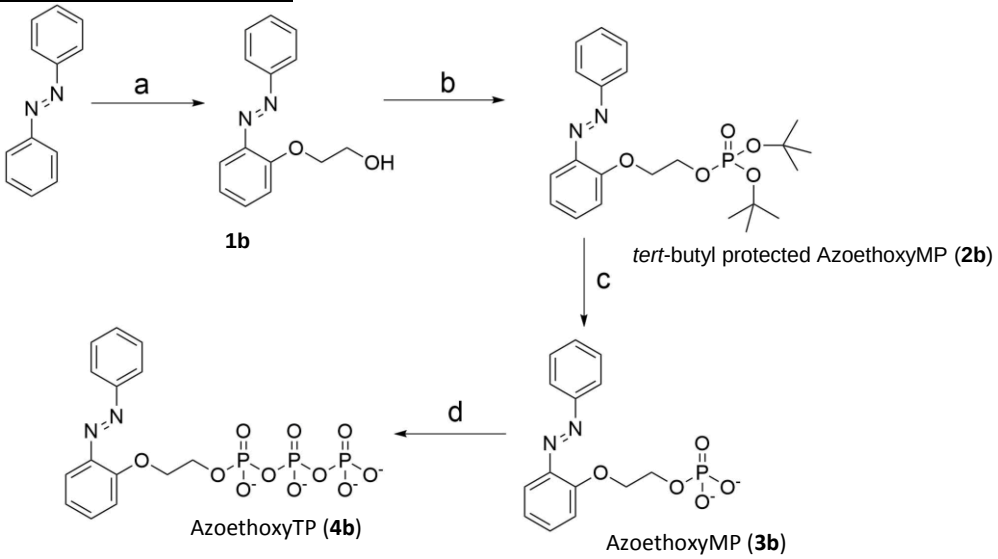

a) Ethylene glycol, $Pd(OAc)_2$, $PhI(OAc)_2$

b) di-*tert*-butyl *N*,*N*-diisopropylphosphoramidite, 1*H*-tetrazole, dry THF, Ar atmosphere, rt, 6h; then, mCPBA,0°C, 1h; then rt, 40 min;

c) Trifluoroacetic acid, dry CH_2Cl_2, Ar atmosphere, rt, 6 h; then eluting through DEAE Sephadex A-25 anion exchanger, TEAB;

d) Tributylamine, carbonyldiimidazole, pyrophosphate, dry DMF, Ar atmosphere, rt, overnight.

Scheme of DimethylAzoTP (4c)

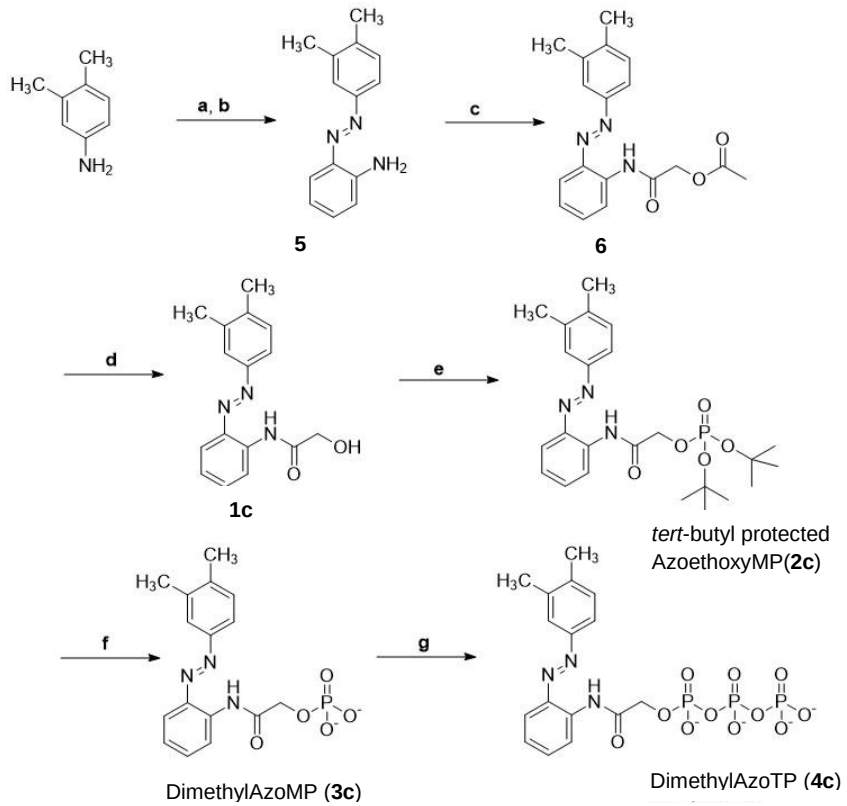

(a) mCPBA, EtOAc, 0°C, 3h.

(b) 1,2-phenylenediamine, AcOH, EtOAc, N_2- atmosphere, 50 °C, 72h.

(c) Acetoxyactyl chloride, Triethylamine, DCM, RT, 3h.

(d) K_2CO_3, MeOH, RT, Overnight.
(e) Di-*tert*-butyl *N*,*N*-Diisopropylphosphoramidite, 1H-tetrazol, dry THF, Ar-atmosphere, RT, 6h, then mCPBA, 0°C,1h.
(f) TFA, dry DCM, Ar-atmosphere, RT, 6h.
(g) Tributylamine, carbonyldiimidazole, tributylammonium pyrophosphate, dry DMF, Ar-atmosphere, RT, overnight.

Scheme of AzoethylTP (4)

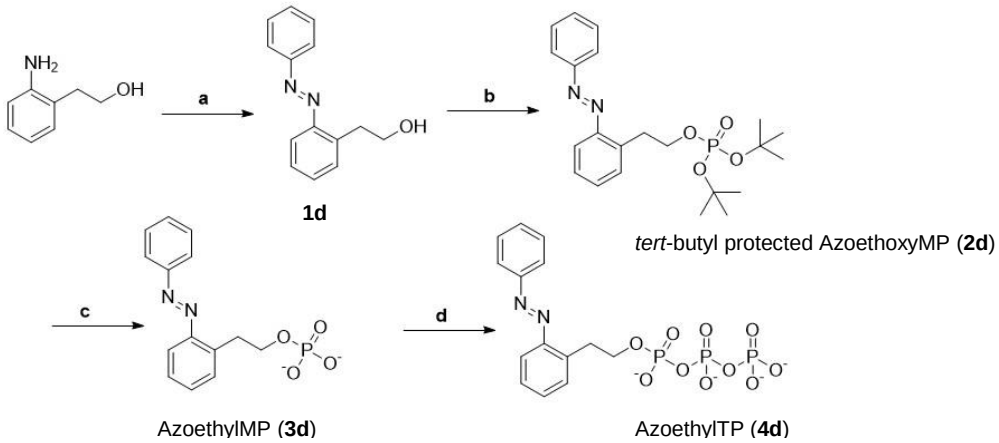

(a) ArNO, AcOH, Toluene, Ar-atmosphere, 60 °C, 72h.
(b) Di-*tert*-butyl *N*,*N*-Diisopropylphosphoramidite, 1H-tetrazol, dry THF, Ar-atmosphere, RT, 6h, then mCPBA, 0°C, 1h.
(c) TFA, dry DCM, Ar-atmosphere, RT, 6h.
(d) Tributylamine, carbonyldiimidazole, tributylammonium pyrophosphate, dry DMF, Ar atmosphere, RT, overnight.

2. Photoisomerization of AzoTPs.

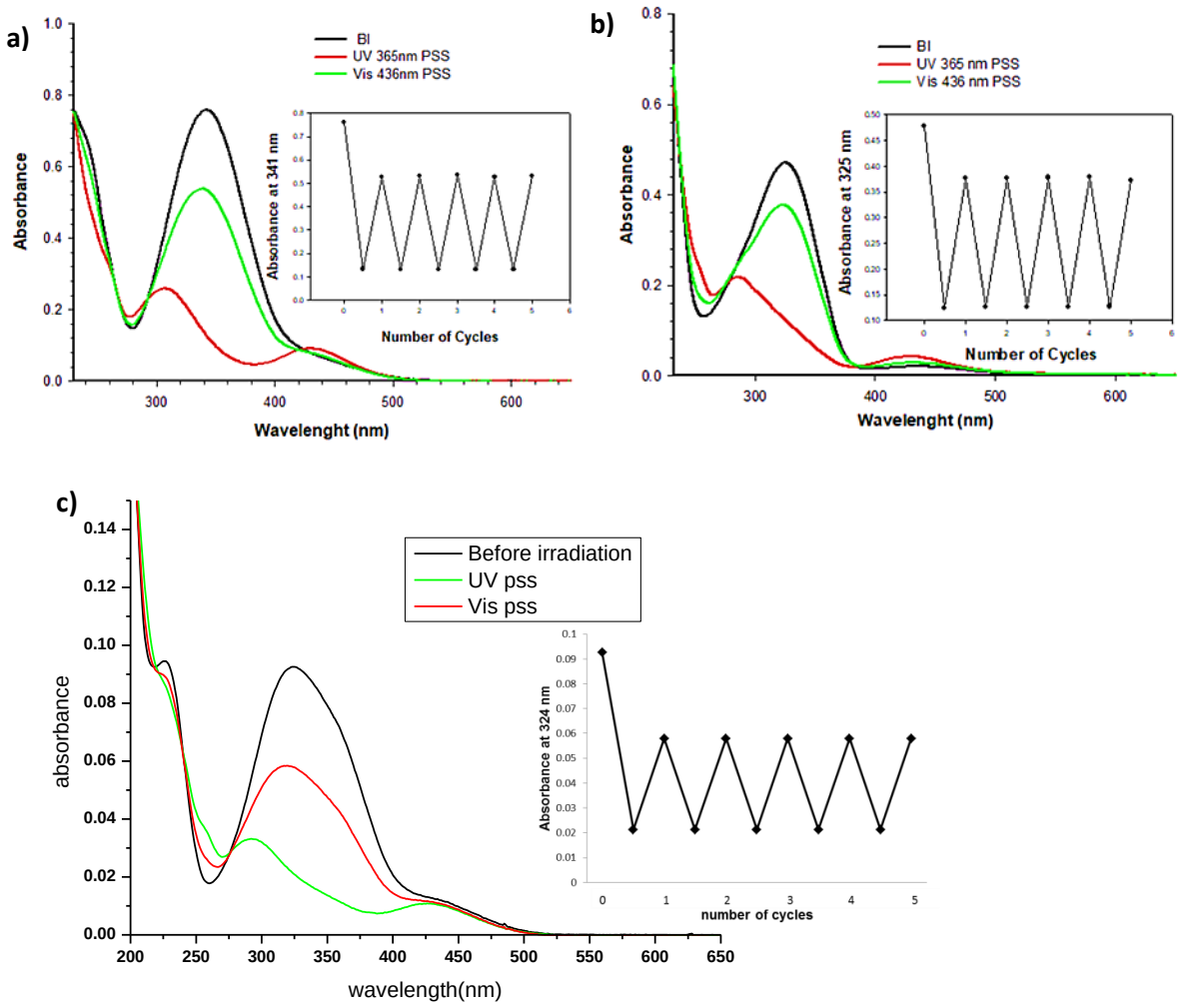

Fig. S1. UV-Vis absorption spectra of AzoTP molecules **a)**DimethylAzoTP (**4c**), **b)** AzoethylTP (**4d**) in BRB-80 buffer solution at 25 °C; before irradiation (black line), UV PSS (red line), Vis PSS (green line) and **c)** AzoethoxyTP (**4b**) in water at 25 °C, before irradiation (black line), UV PSS (green line), Vis PSS (red line). Insets show the absorbance changes a) at 341 nm, b) at 325 nm and c) at 324 nm after the alternate irradiations by 365 and 436 nm light for 5 cycles.

3. Isomerization ratio of *cis* and *trans* at UV and Visible PSS

The photo conversion ratio from *trans* to *cis and cis* to *trans* isomers of the AzoTPs corresponding to irradiation with 365 nm and 436 nm light was measured with ^{1}H NMR (400 MHz, D_2O).

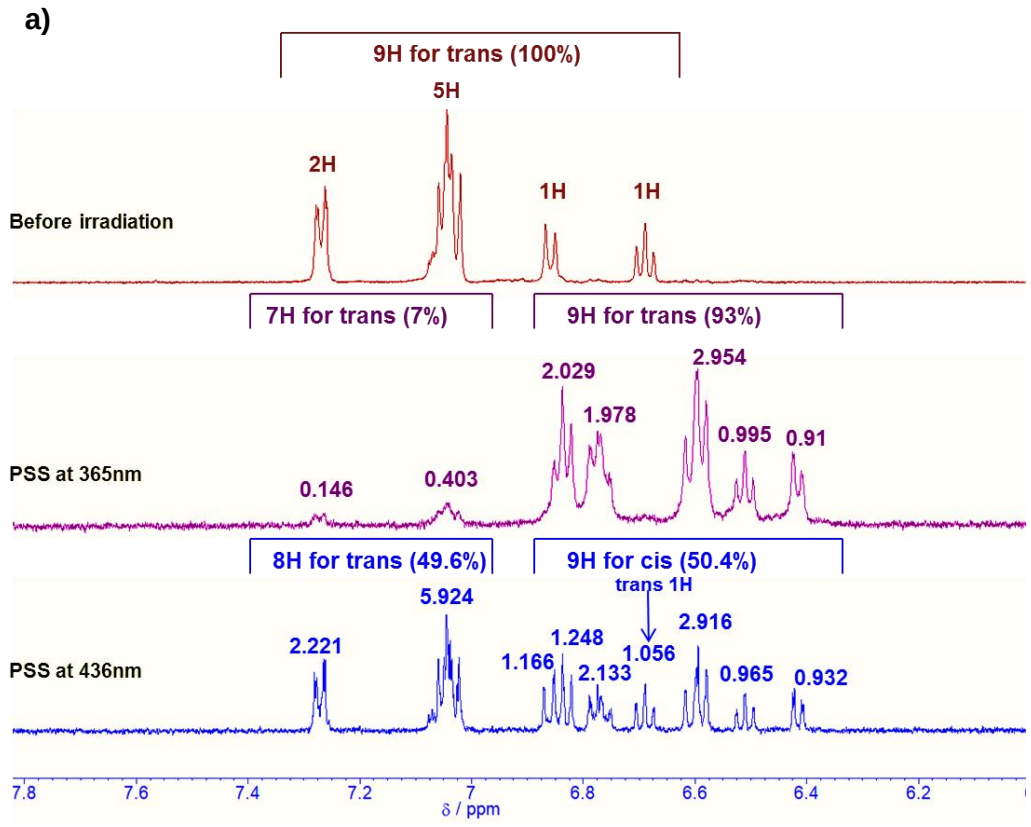

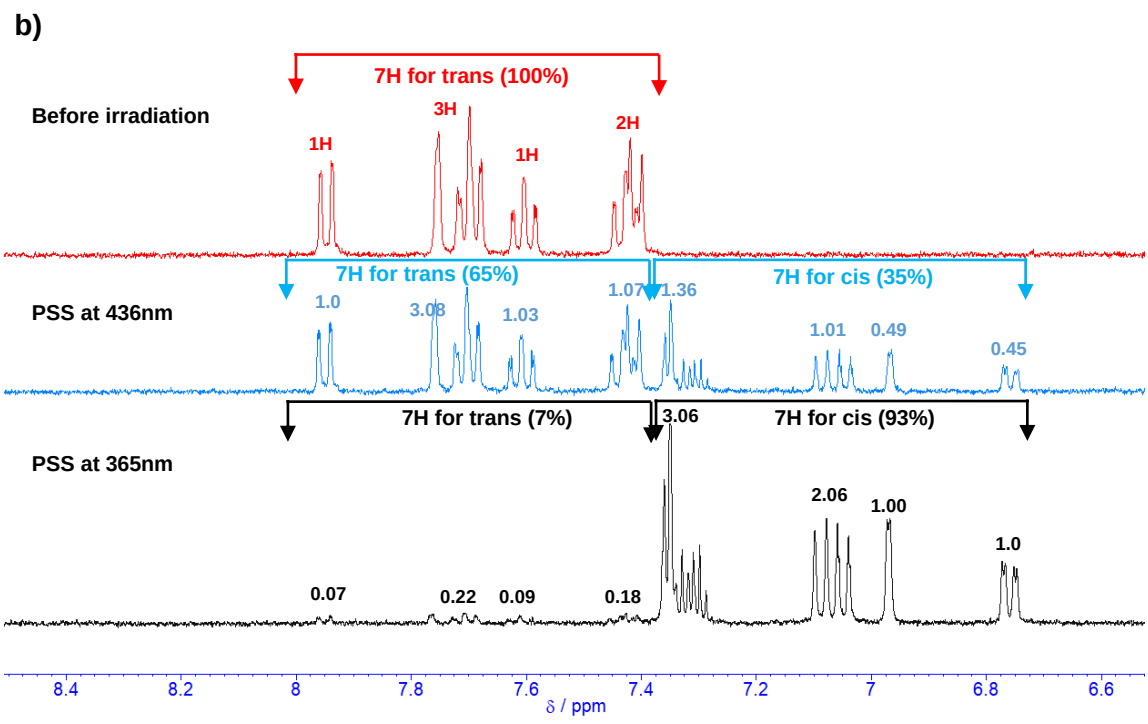

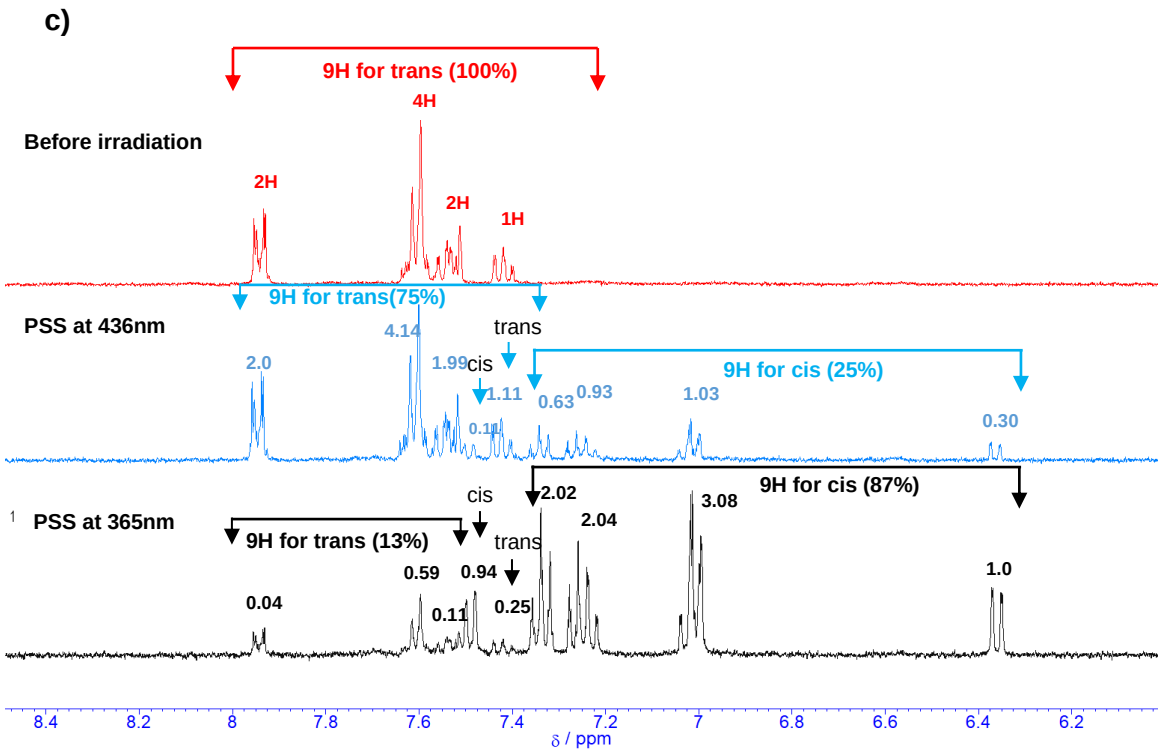

Fig. S2. ^{1}H NMR spectra (400 MHz, D_2O) showing the *trans* and *cis* isomer ratios of **a)** AzoethoxyTP (**4b**), **b)** DimethylAzoTP (**4c**) and **c)** AzoethylTP (**4d**) before irradiation, at UV PSS and Visible PSS.

4. Muscle fibre shortening as a function of AzoTP concentration

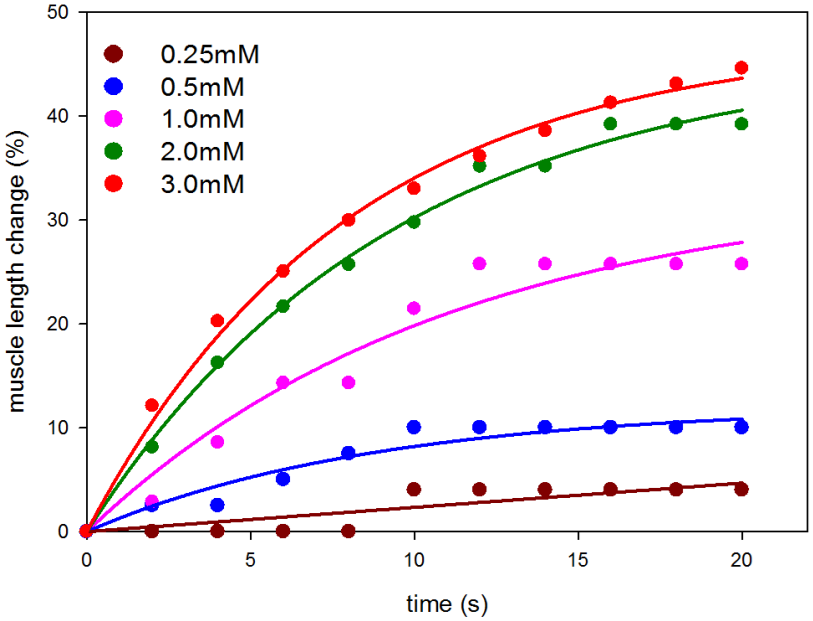

Fig. S3. AzoTP (**4a**) concentration dependent shortening of muscle fiber. Lines are best fit through the data trend.

5. Purity of the AzoTPs by HPLC analysis.

a)

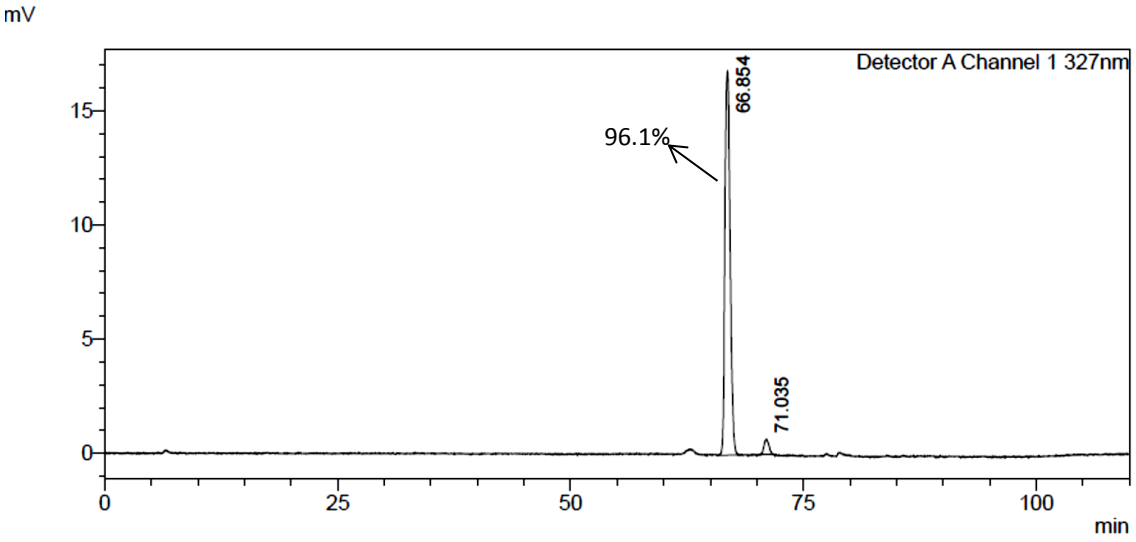

b)

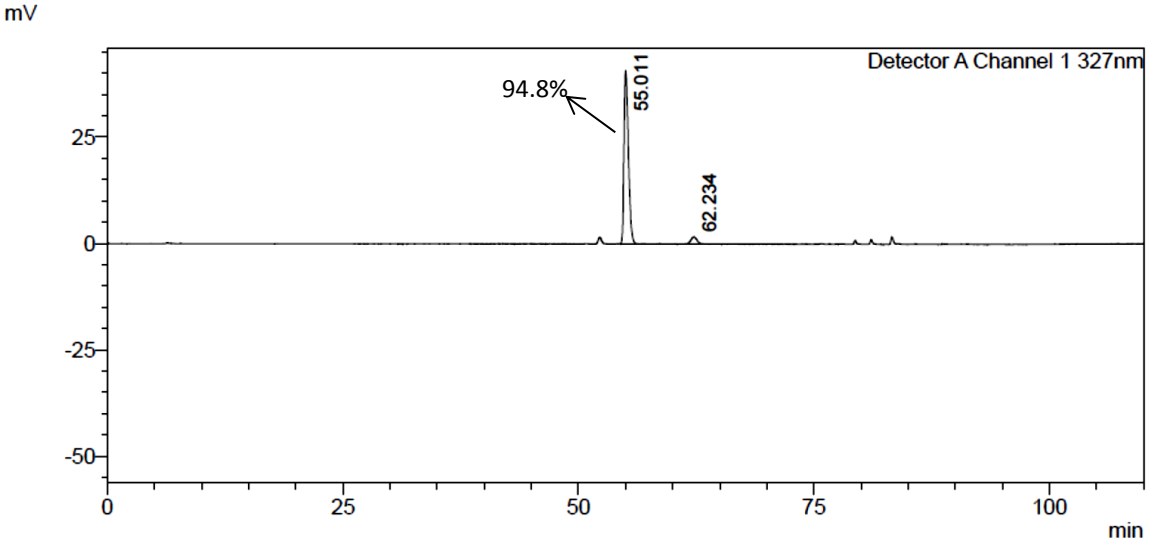

c)

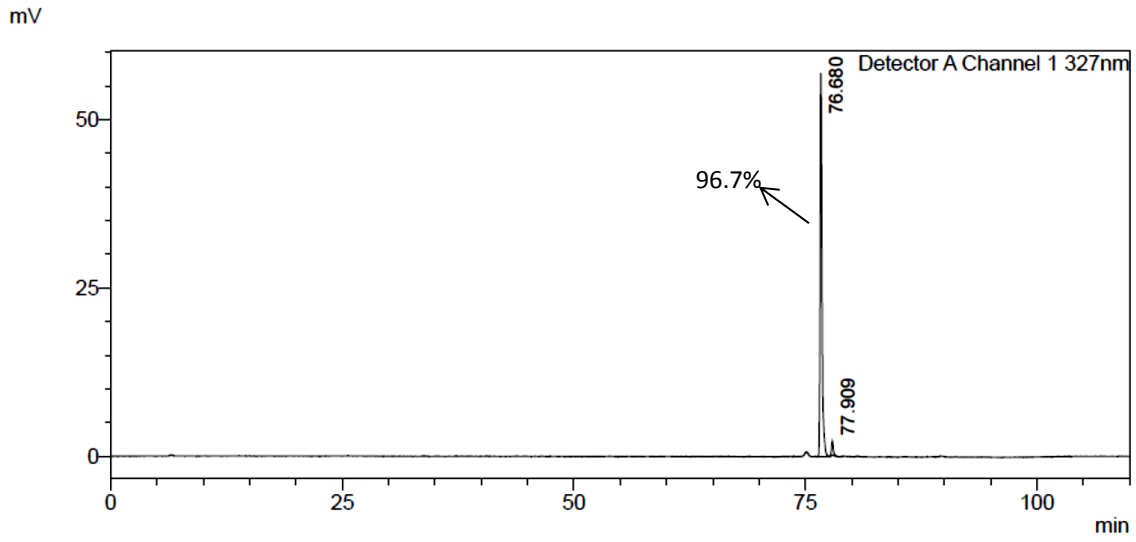

d)

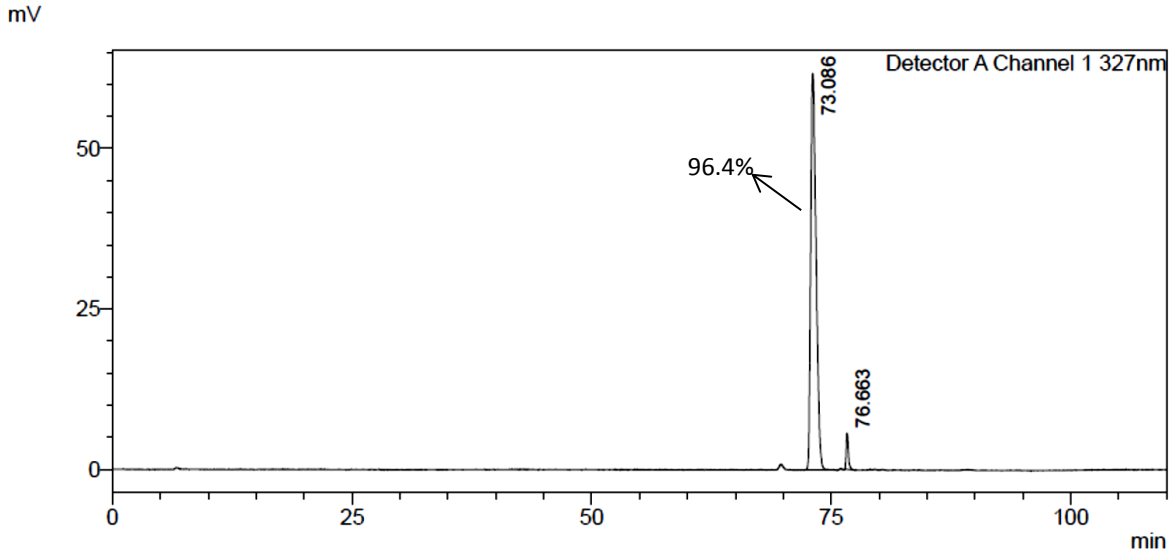

Fig. S4. Reverse phase HPLC chromatograms of **a**) AzoTP (**4a**), **b**) AzoethoxyTP (**4b**), **c**) DimethylAzoTP (**4c**), **d**) AzoethylTP (**4d**) showing > 95% purity. Conditions of the RP-HPLC analysis; Column: CN-80Ts, 4.6 × 250 mm (TOSOH). Eluent: Eluent - CH_3CN/NaPi buffer (pH 6.5). Solvent gradient: 15 – 45% of CH_3CN in NaPi buffer. Monitoring wavelength: λ = 327 nm. Flow rate: 0.5 mL/min at room temperature (23 °C). Injection volume: 20 μL.

6. Mass spectra of AzoTP molecules.

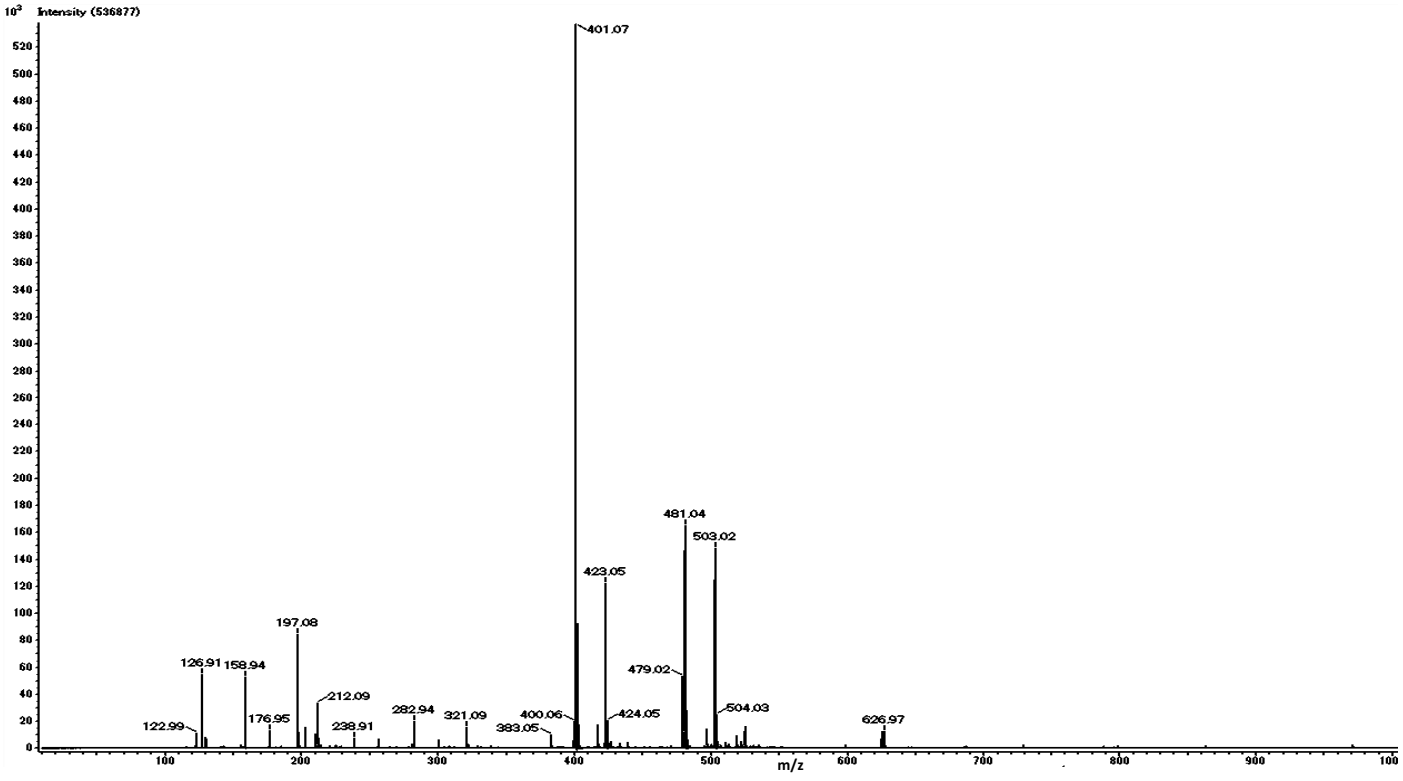

Fig. S5. ESI mass spectrum of AzoethoxyTP (**4b**), the peaks at *m/z* = 504.03, 503.02, 479.02 and 481.04 assigned to the $[M\text{-}H]^-$ ions of monosodium tetraprotonated, monosodium triprotonated, diprotonated and tetraprotonated AzoethoxyTP species respectively. The peaks at *m/z* = 424.05, 423.05 and 401.07 assigned to $[M\text{-}H]^-$ ions of monosodium triprotonated, monosodium diprotonated and triprotonated AzoethoxyDP species respectively.

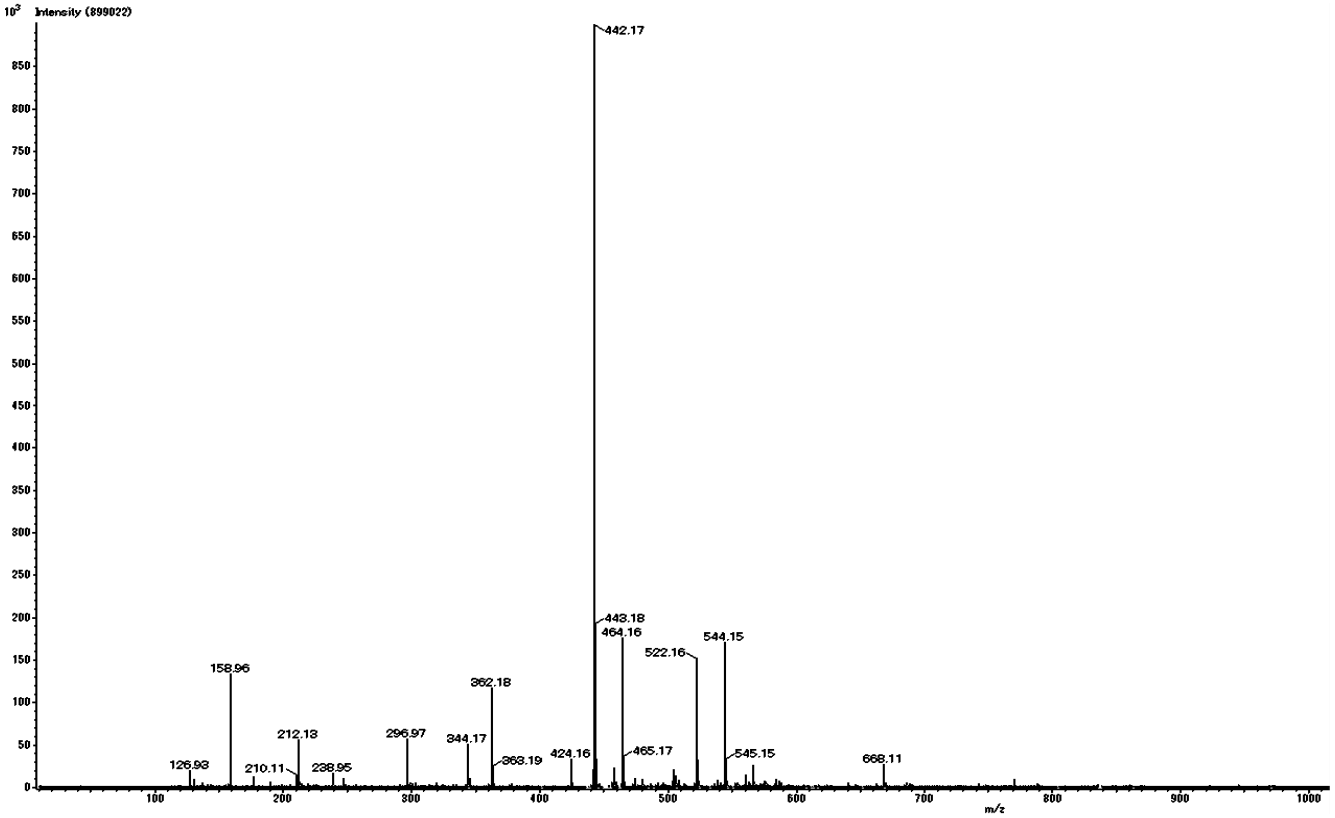

Fig. S6. ESI mass spectrum of DimethylAzoTP (**4c**), the peaks at *m*/*z* = 668.11, 544.15 and 522.16 can be assigned to the $[M-H]^-$ ions of disodium-mono triethyl ammonium, monosodium and tetra-protonated DimethylAzoTP species respectively. The peaks at *m*/*z* = 464.16 and 442.17 can be assigned to the $[M-H]^-$ ions of monosodium and tri-protonated DimethylAzoDP species respectively.

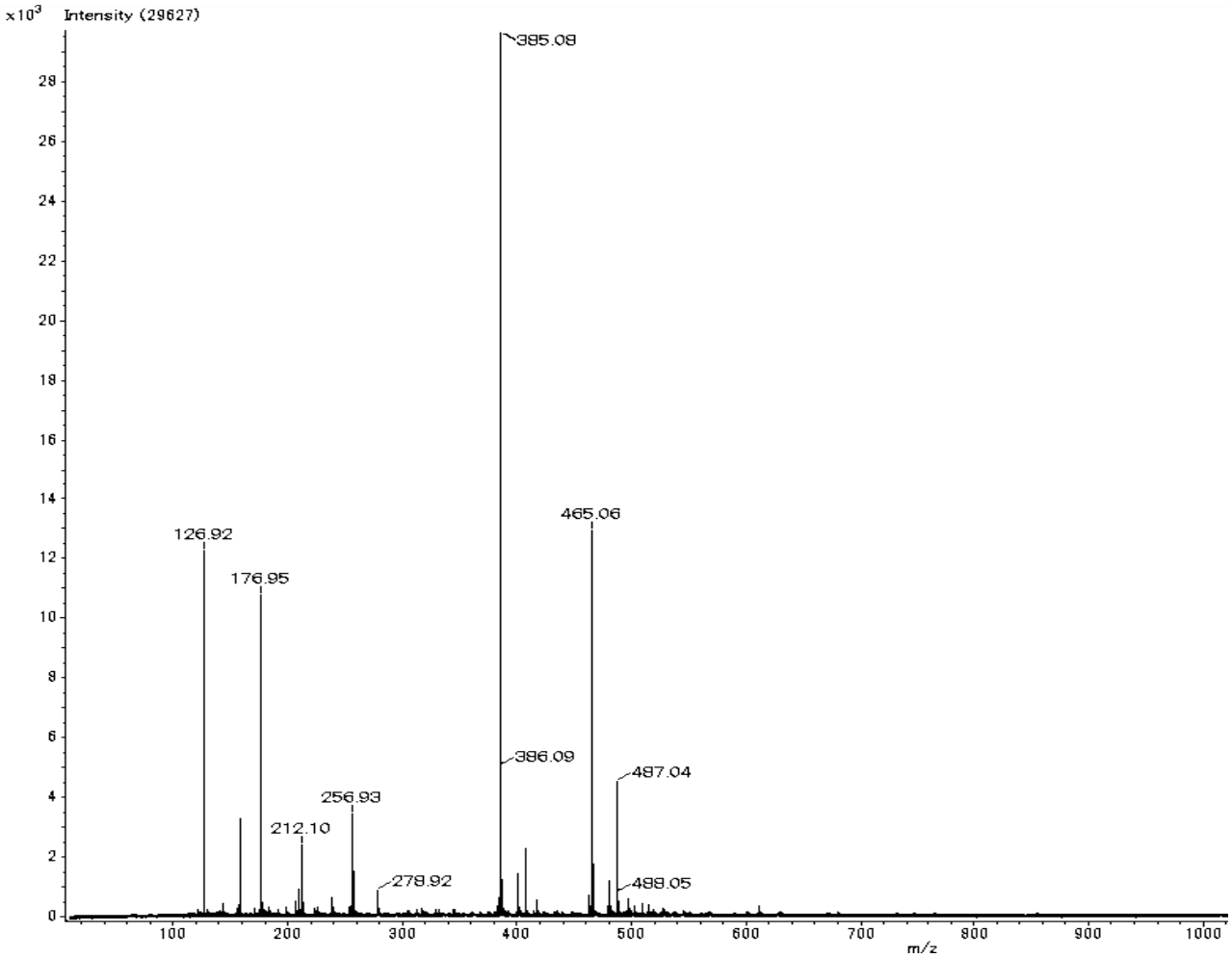

Fig. S7. ESI mass spectrum of AzoethylTP (**4d**), the peaks at *m/z* = 487.04, 465.06 and 385.08 can be assigned to the $[M-H]^-$ ions of monosodium, tetra-protonated AzoethylTP and tri-protonated AzoethylDP species respectively.

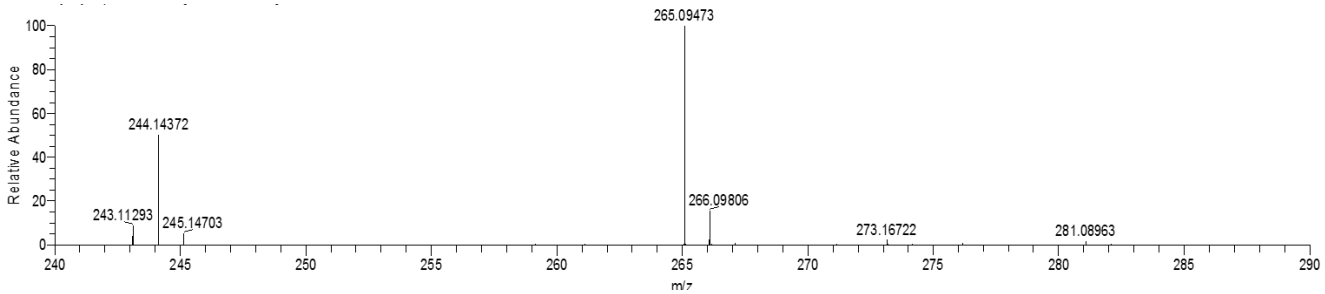

Fig. S8. High-resolution mass spectrum of **1b** calculated for $C_{14}H_{16}N_2O_2Na$ $[M + Na]^+$: 265.09475

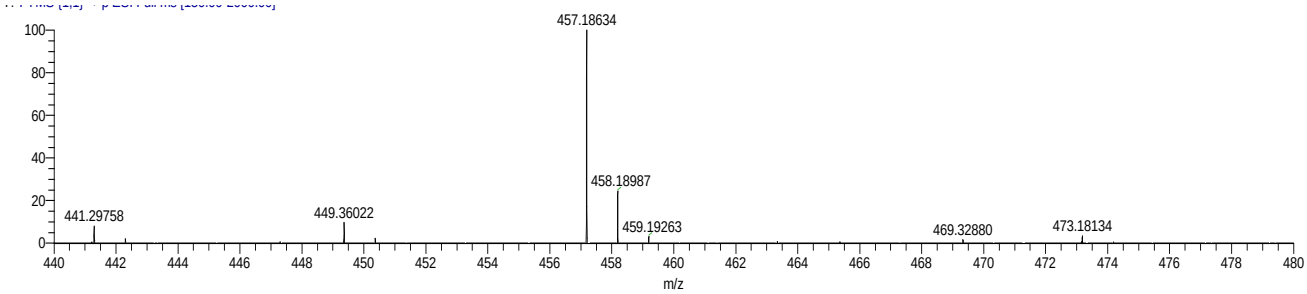

Fig. S9. High-resolution mass spectrum of **2b** calculated for $C_{22}H_{31}N_2O_5PNa$ $[M + Na]^+$: 457.18628.

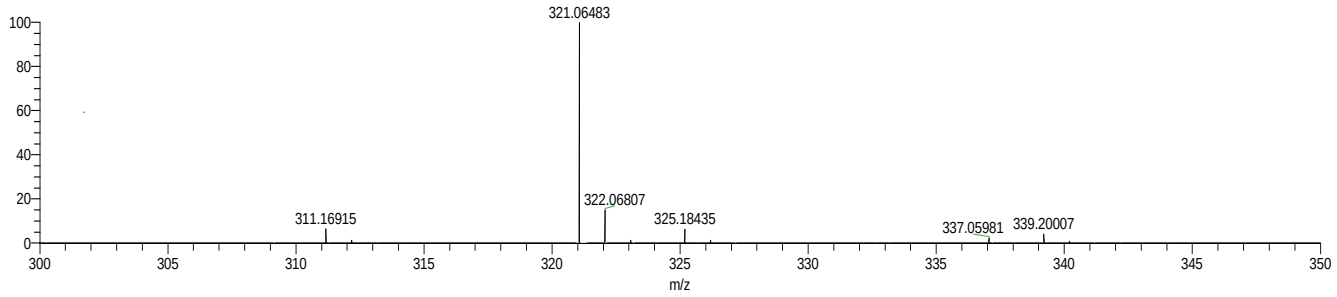

Fig. S10. High-resolution mass spectrum of **3b** calculated for $C_{14}H_{14}N_2O_5P$ $[M - H]^-$: 321.06458.

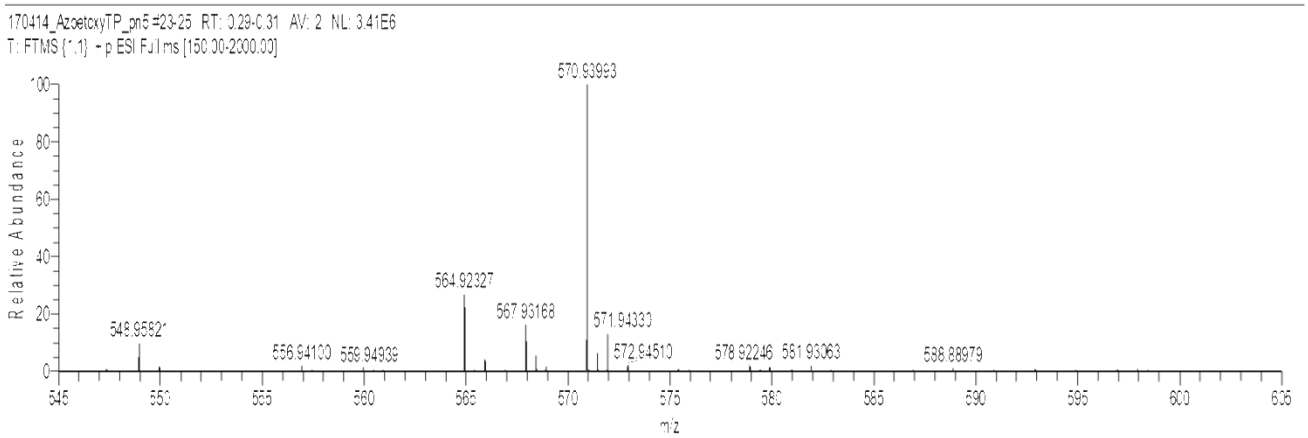

Fig. S11. High-resolution mass spectrum of AzoethoxyTP (**4b**) as tetrasodium salt calculated for $C_{14}H_{14}N_2O_{11}Na_4P_3$ $[M + H]^+$: 570.93957

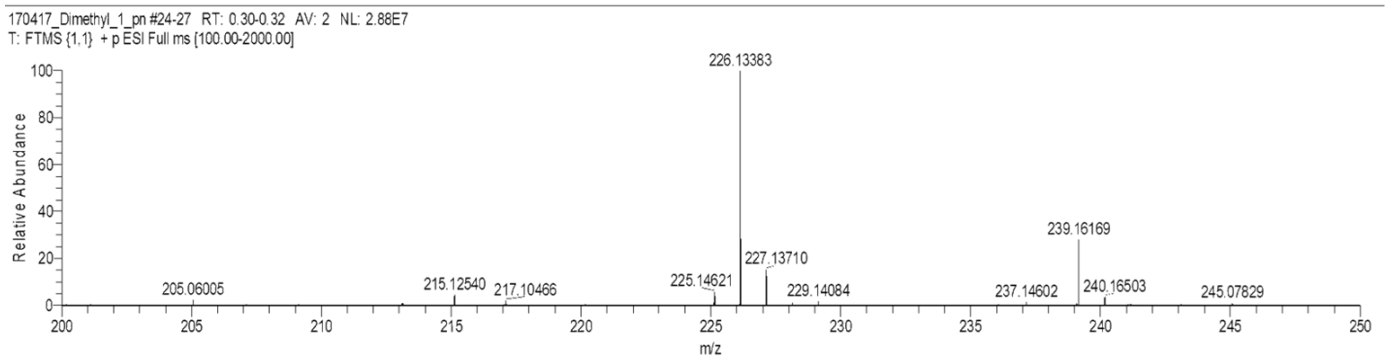

Fig. S12. High-resolution mass spectrum of **5** calculated for $C_{14}H_{16}N_3$ $[M + H]^+$: 226.13387.

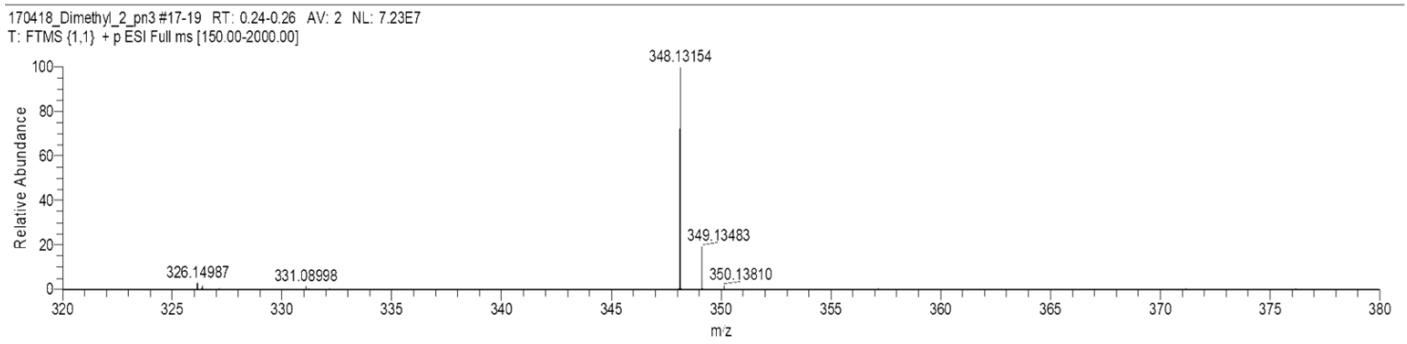

Fig. S13. High-resolution mass spectrum of **6** calculated for $C_{18}H_{19}N_3O_3Na$ $[M + Na]^+$: 348.13186.

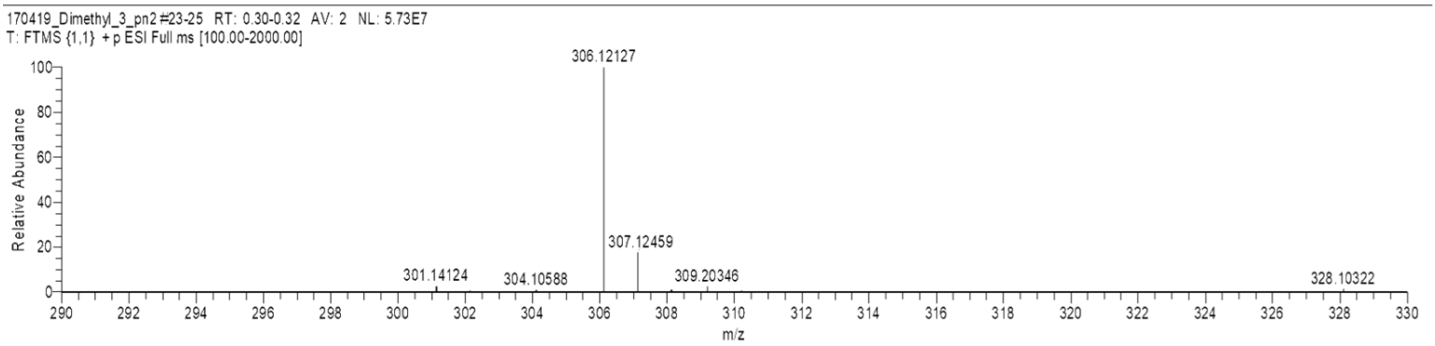

Fig. S14. High-resolution mass spectrum of **1c** calculated for $C_{16}H_{17}N_3O_2Na$ $[M + Na]^+$: 306.12130.

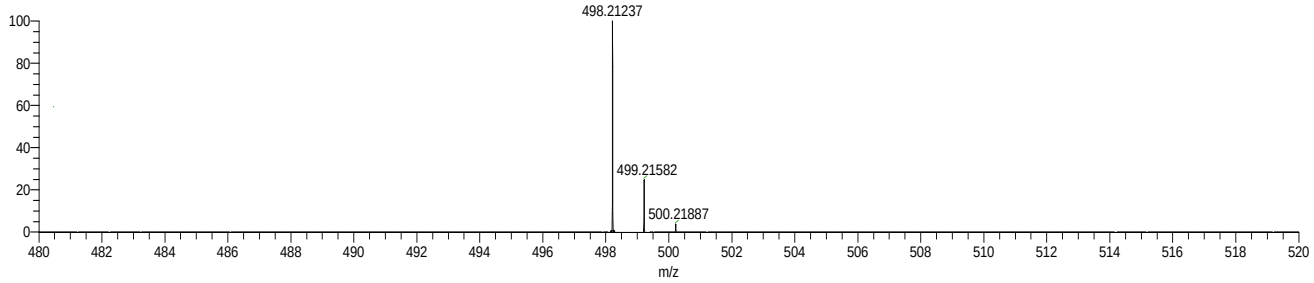

Fig. S15. High-resolution mass spectrum of **2c** calculated for $C_{24}H_{34}N_3O_5P$ $[M + Na]^+$: 498.21283.

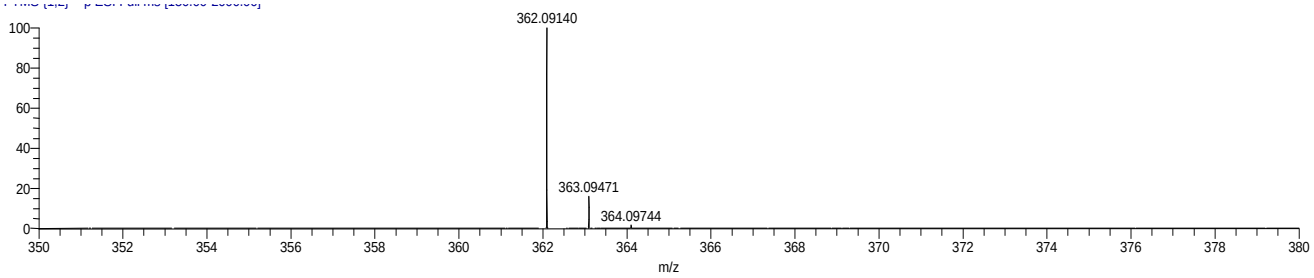

Fig. S16. High-resolution mass spectrum of **3c** calculated for $C_{16}H_{17}N_3O_5P$ $[M – C_6H_{17}N(TEA)]^-$:362.09113.

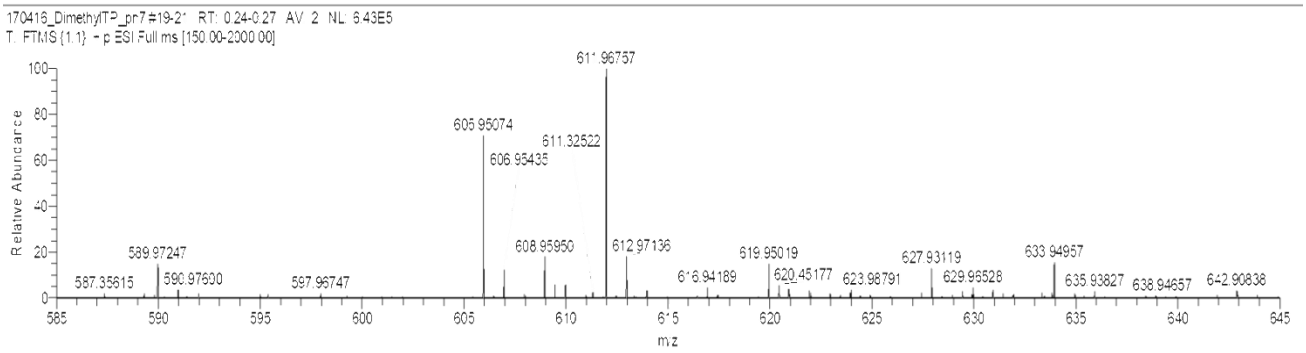

Fig. S17. High-resolution mass spectrum of DimethylAzoTP (**4c**) as tetrasodium salt calculated for $C_{16}H_{16}N_3O_{11}Na_4P_3$ $[M + H]^+$: 611.96612.

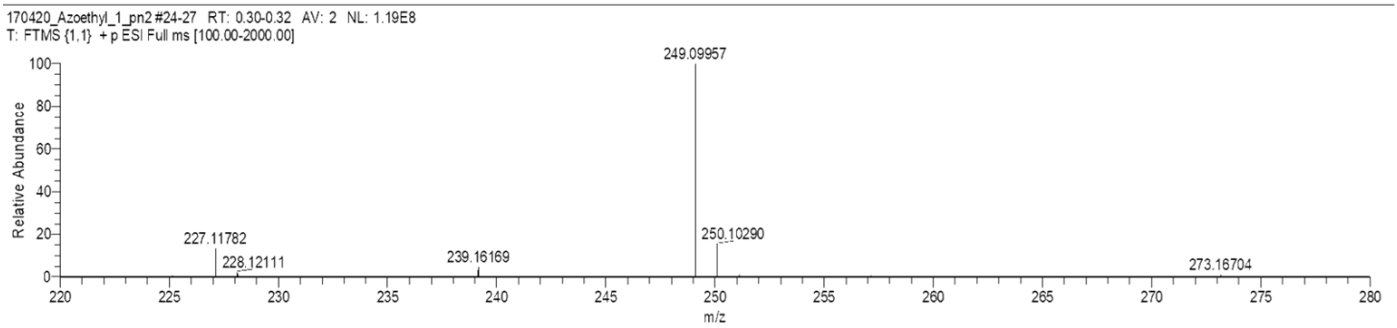

Fig. S18. High-resolution mass spectrum of **1d** calculated for $C_{14}H_{14}N_2ONa$ $[M + Na]^+$: 249.09983.

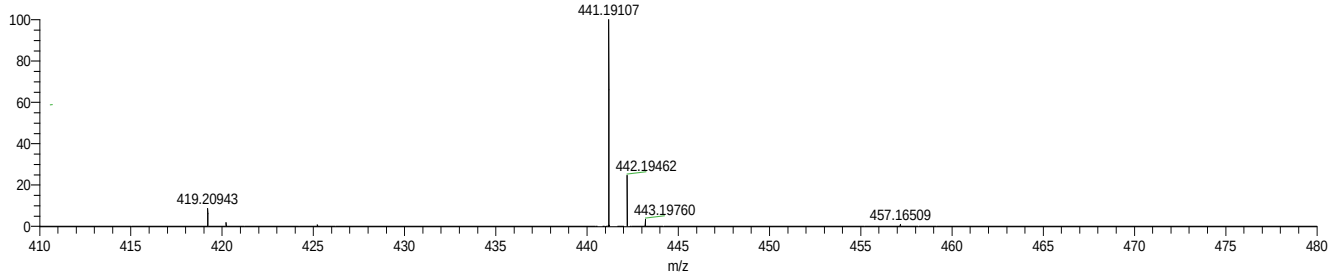

Fig. S19. High-resolution mass spectrum of **2d** calculated for $C_{22}H_{31}N_2O_4PNa$ $[M + Na]^+$: 441.19137.

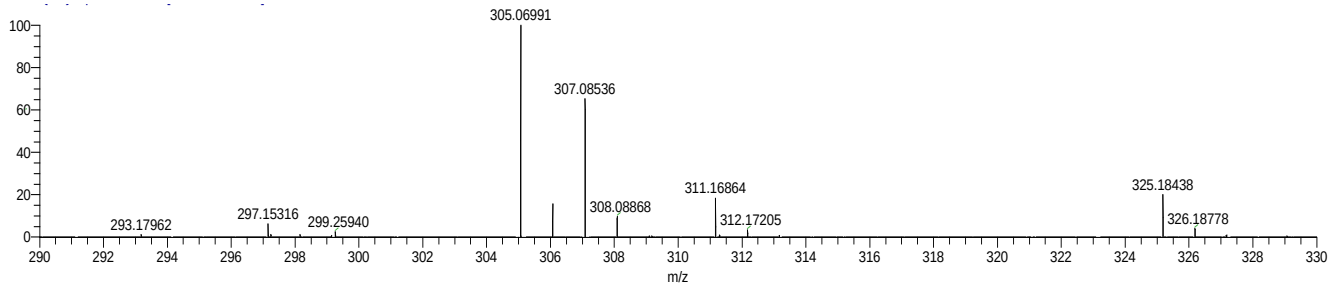

Fig. S20. High-resolution mass spectrum of **3d** $C_{14}H_{14}N_2O_4P$ $[M - C_6H_{16}N(TEA)]^-$: 305.06967.

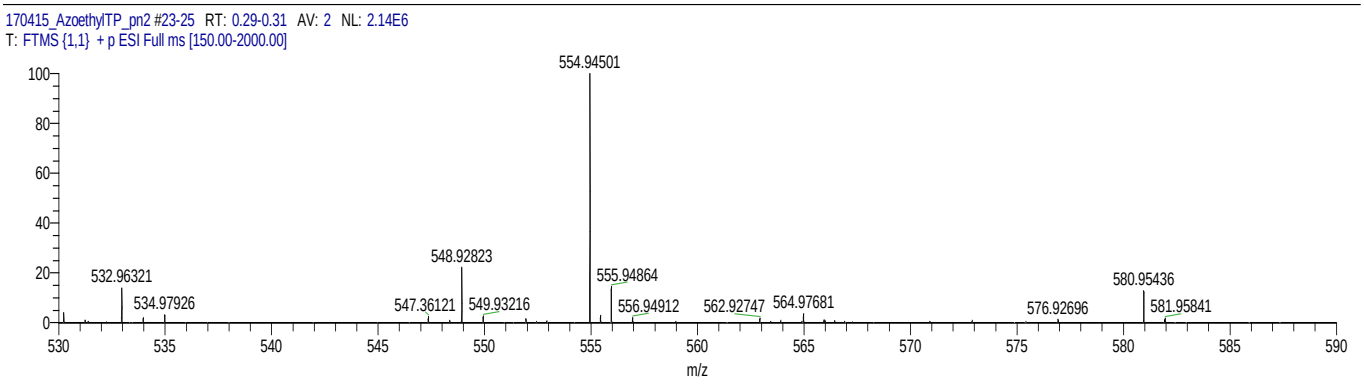

Fig. S21. High-resolution mass spectrum of AzoethylTP (**4d**) as tetrasodium salt calculated for $C_{14}H_{14}N_2O_{10}Na_4P_3$ $[M + H]^+$: 554.94466.

7. Supplementary Movies

Mv01: Movie demonstrates the in-situ photoregulation of F-actin motility by irradiating alternatingly with 365nm(3s) and 510nm (5s). The change in the velocity of fluroscently labelled actin filaments corresponding to the light irradiation could be seen. After UV irradiation the filaments move slowly and after shining Visible light the speed increses drastically. The concentration of **4a** is 40 µM.

Mv02: This movie demonstrates the effect of *trans* and *cis* isomer of **4a** on the glycerinated muscle fibre. *cis*-**4a** was added to one fibre and *trans*-**4a** added to the other. Fibre shortens after addition of *trans*-**4a** solution while the fibre infused with *cis*-**4a** doesn't show any change in the length. *cis*-**4a** was pregenerated before addition on muscle fibre. Concentration of **4a** is 3 mM (total).

Mv03: This movie demonstrates that the photo-induced shortening of muscle fibre is due to the photo-generated *trans* isomer and not due to the heat of irradiation. Buffer solution without any **4a** is added to one fibre and to the fibre *cis*-**4a** is added. Both the fibres don't shorten even in 20s after addition of buffer and *cis*-**4a** solution respectively, unlike as seen in the **Mv01** where the fibre shortens significantly in 20s duration after addition of *trans*-**4a**. So this again reconfirms that *cis*-**4a** doesn't induce muscle fibre shortening. Both the fibres are irradiated with 510nm light for 10s. Muscle fibre infused with *cis*-**4a** shortenes about 38% of its initial length while the buffer solution infused fibre doesn't show any change in the length. Concentration of **4a** is 3 mM (total).

Mv04: This movie demostrates the photoinduced shortening of muscle fibre infused in inactive *cis* –**4a** solution. To both the muscle fibres *cis*-**4a** solution was added and one fibre was irradiated with 510nm light for 10s. The irradiated fibre shortens about 31% of its length before irradiation whereas the non-irradiated muscle fibre exhibits no change in length as shown in the snapshots of the video below.

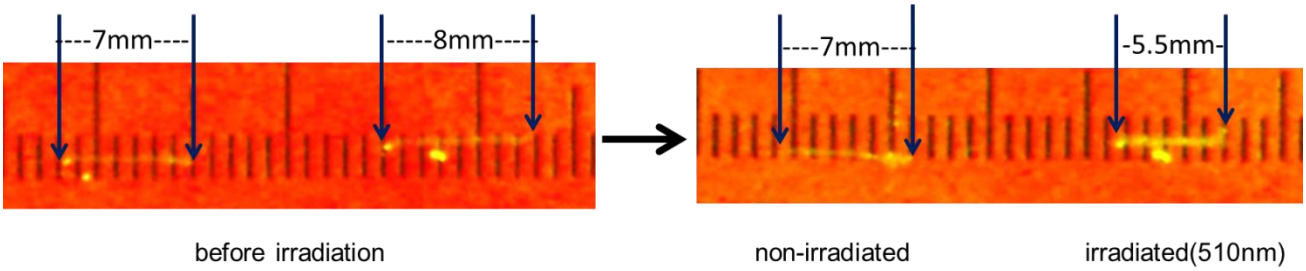

8. NMR spectral data

^{1}H NMR and ^{13}C NMR spectra of **1b**

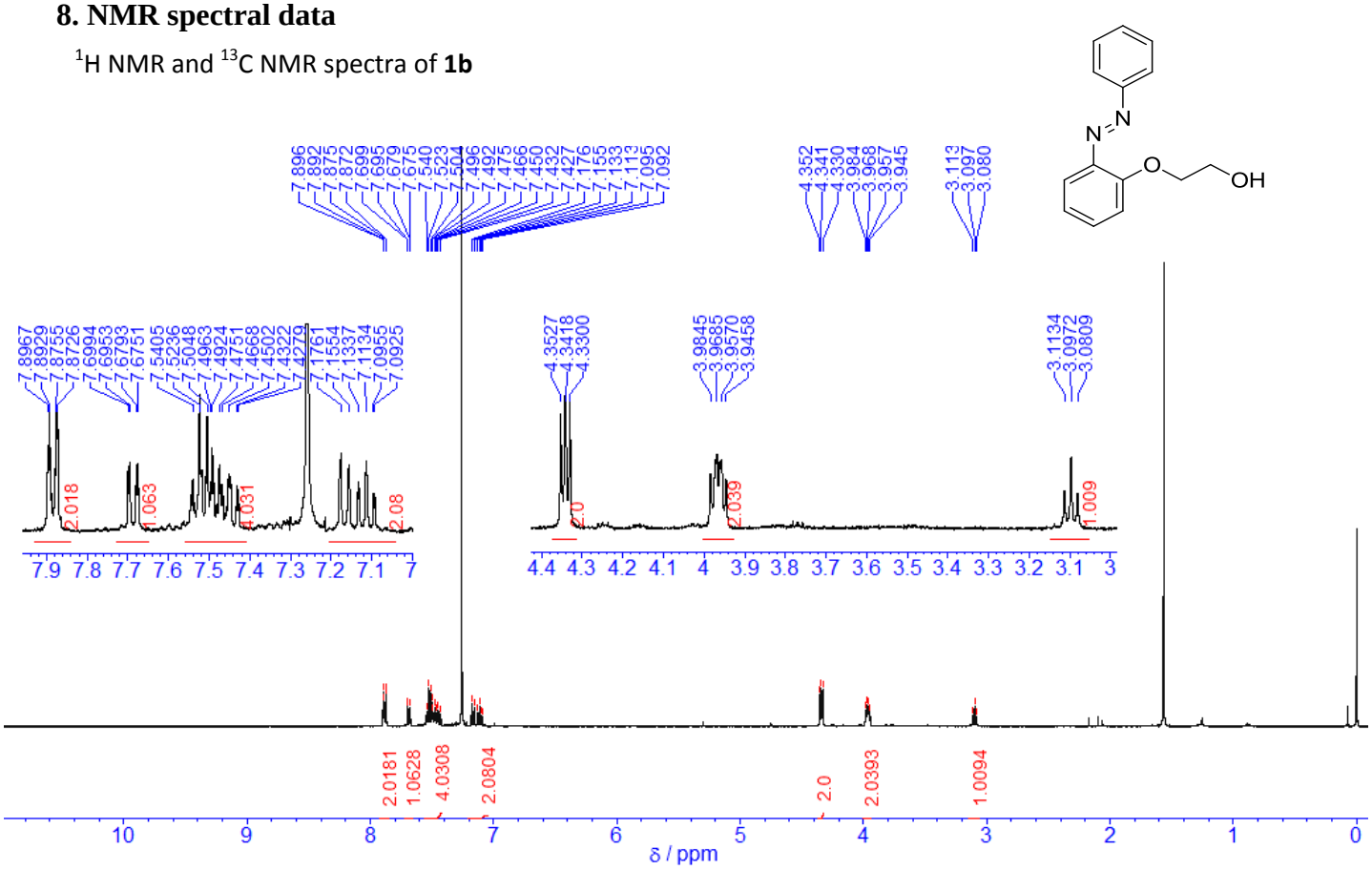

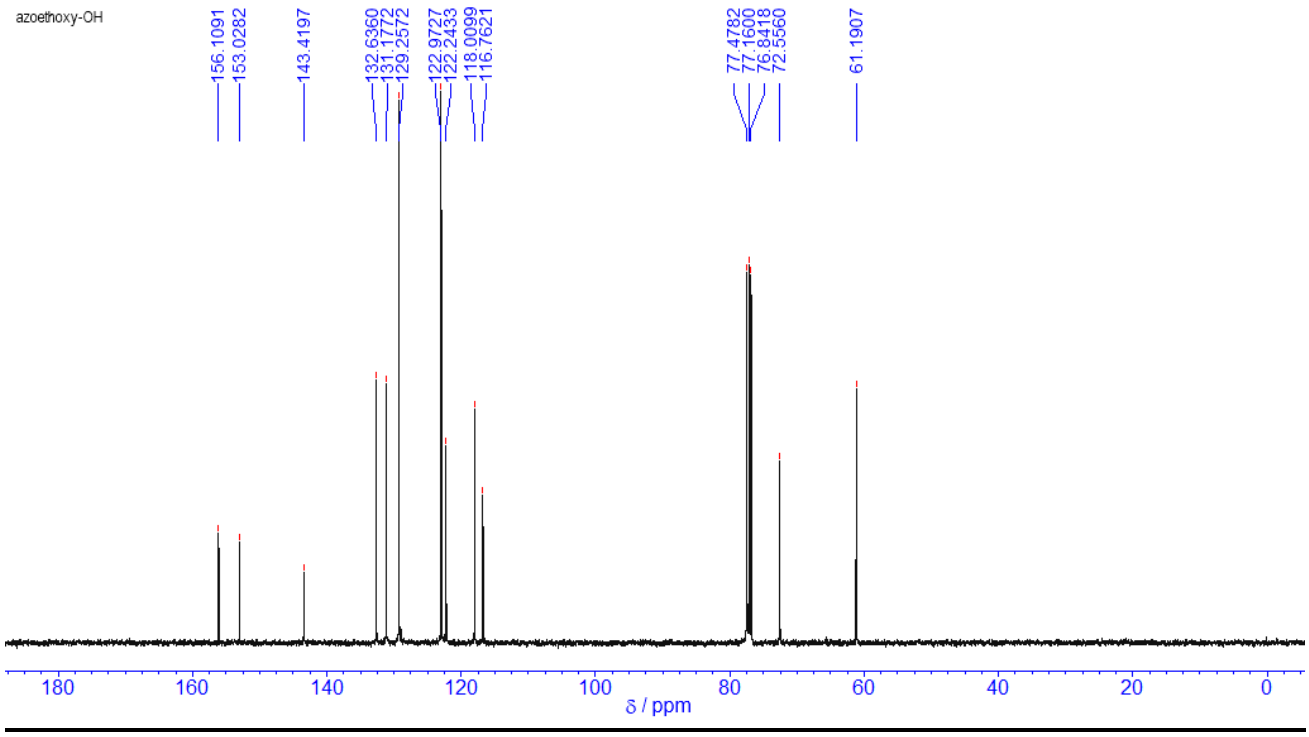

^{1}H NMR and ^{13}C NMR spectra of **2b**

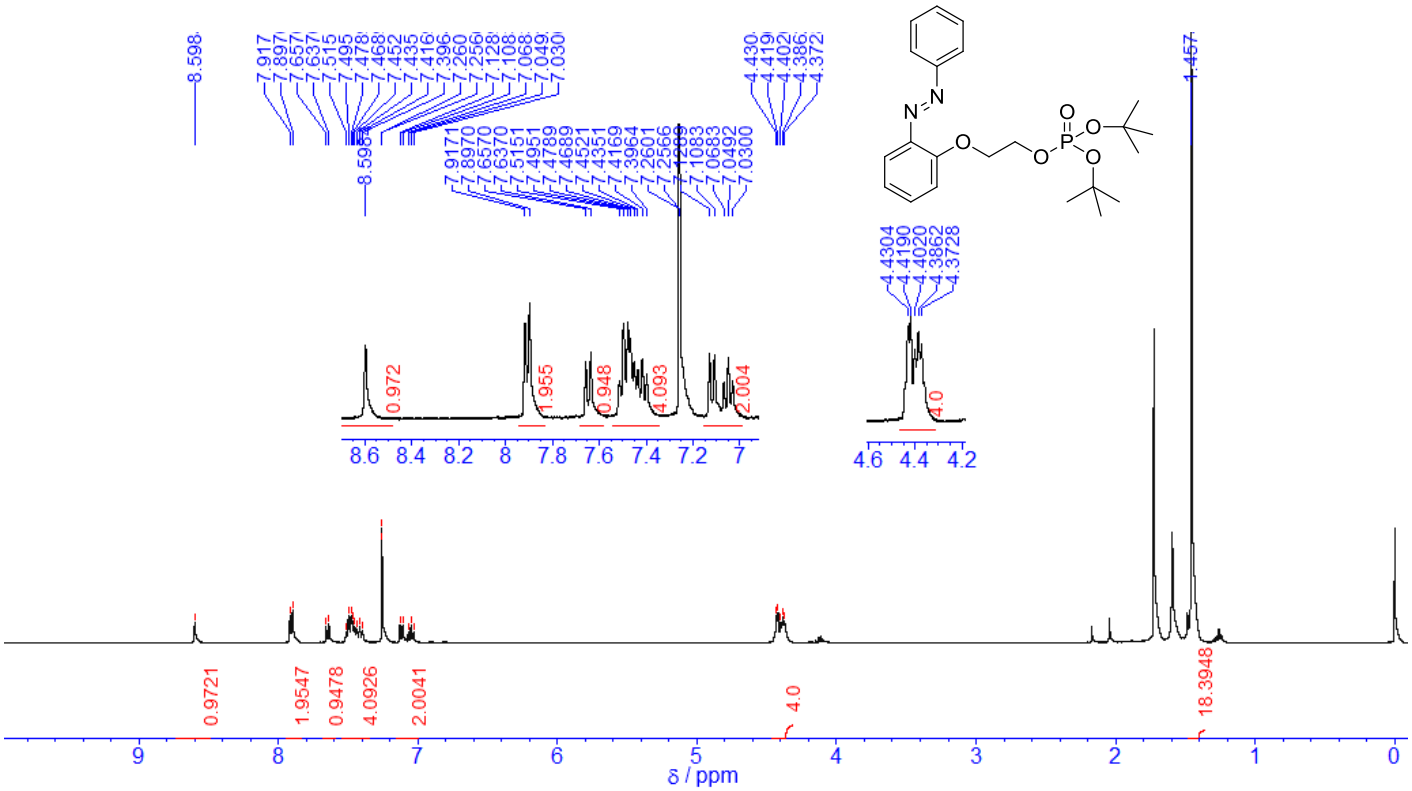

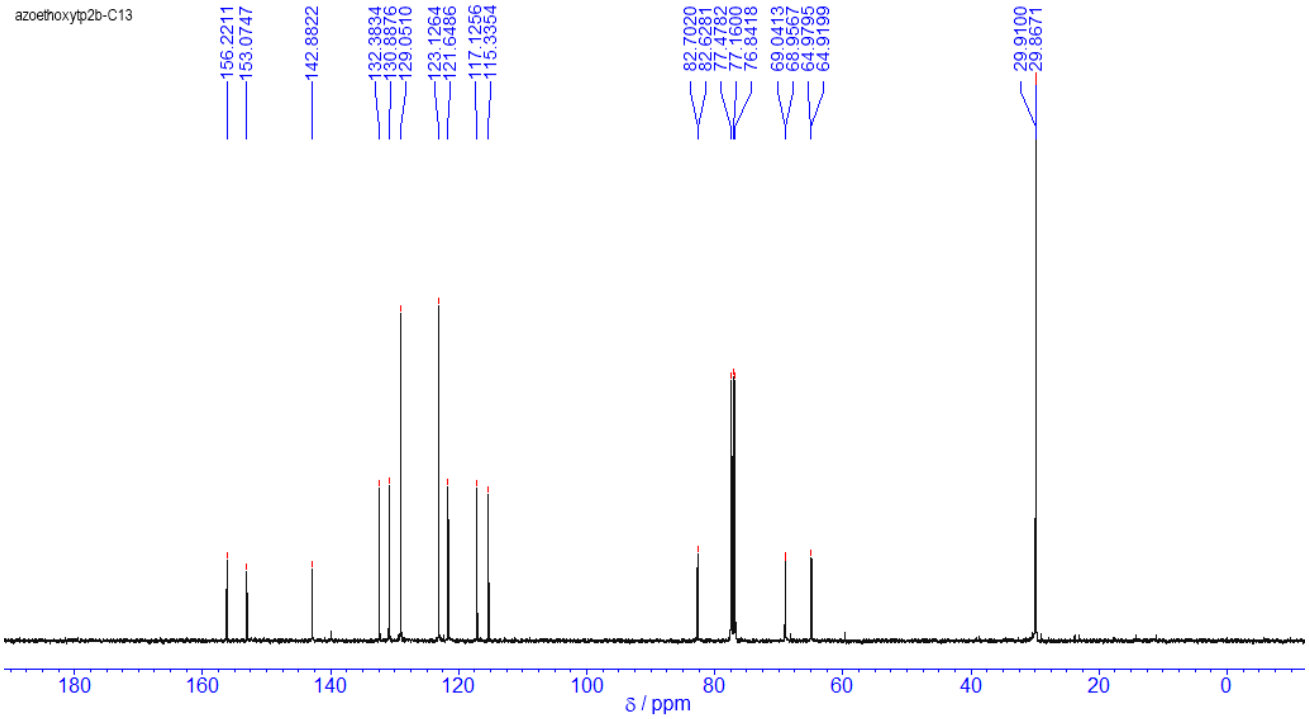

^{1}H NMR and ^{13}C NMR spectra of **3b**

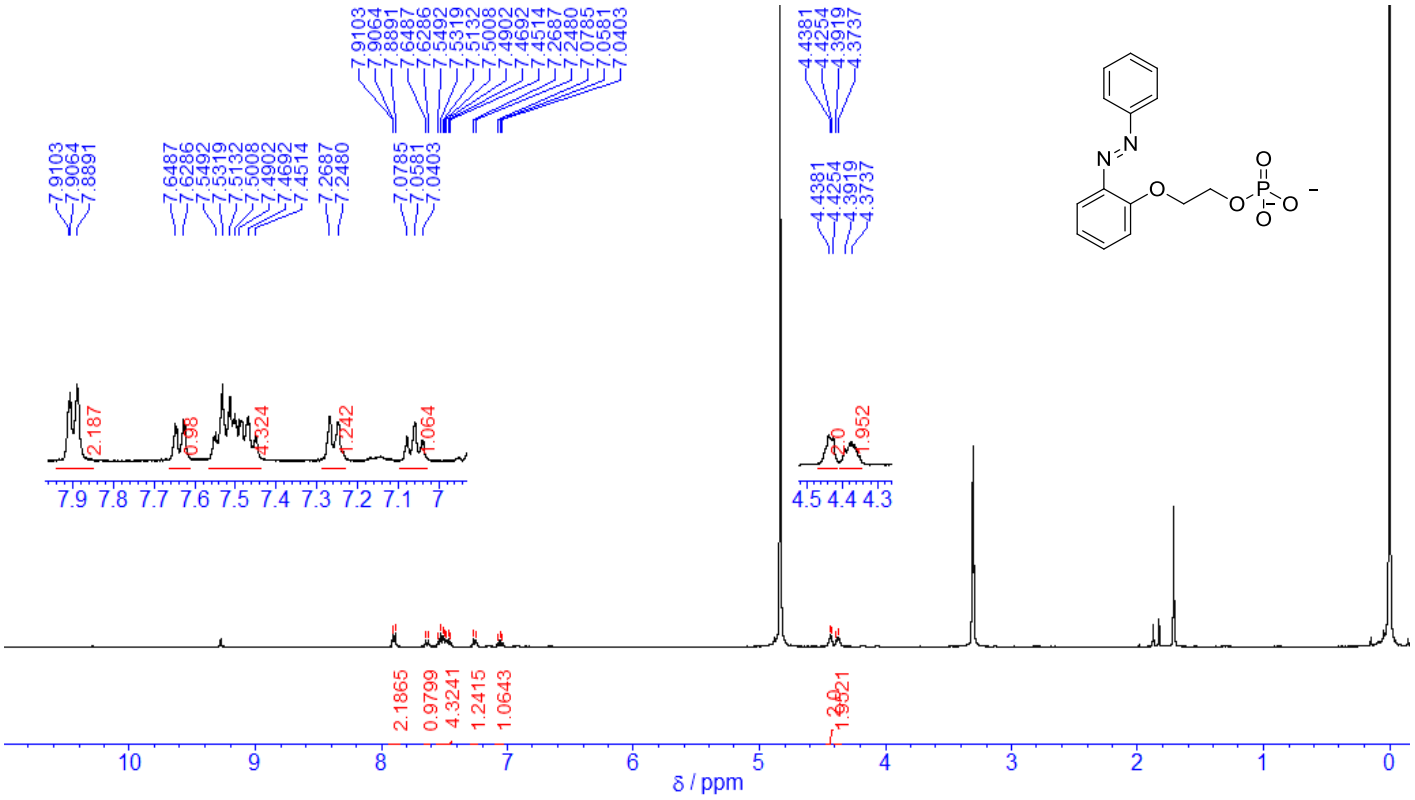

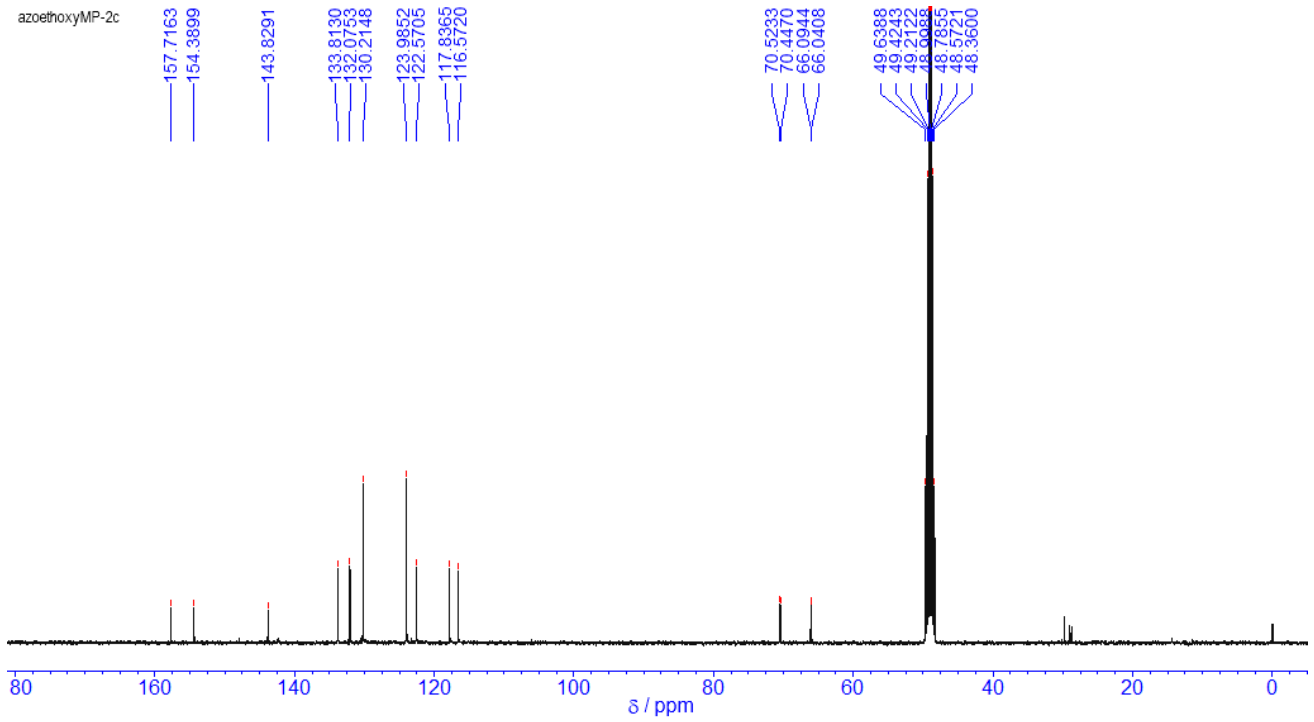

^{1}H NMR and ^{13}C NMR spectra of **4b**

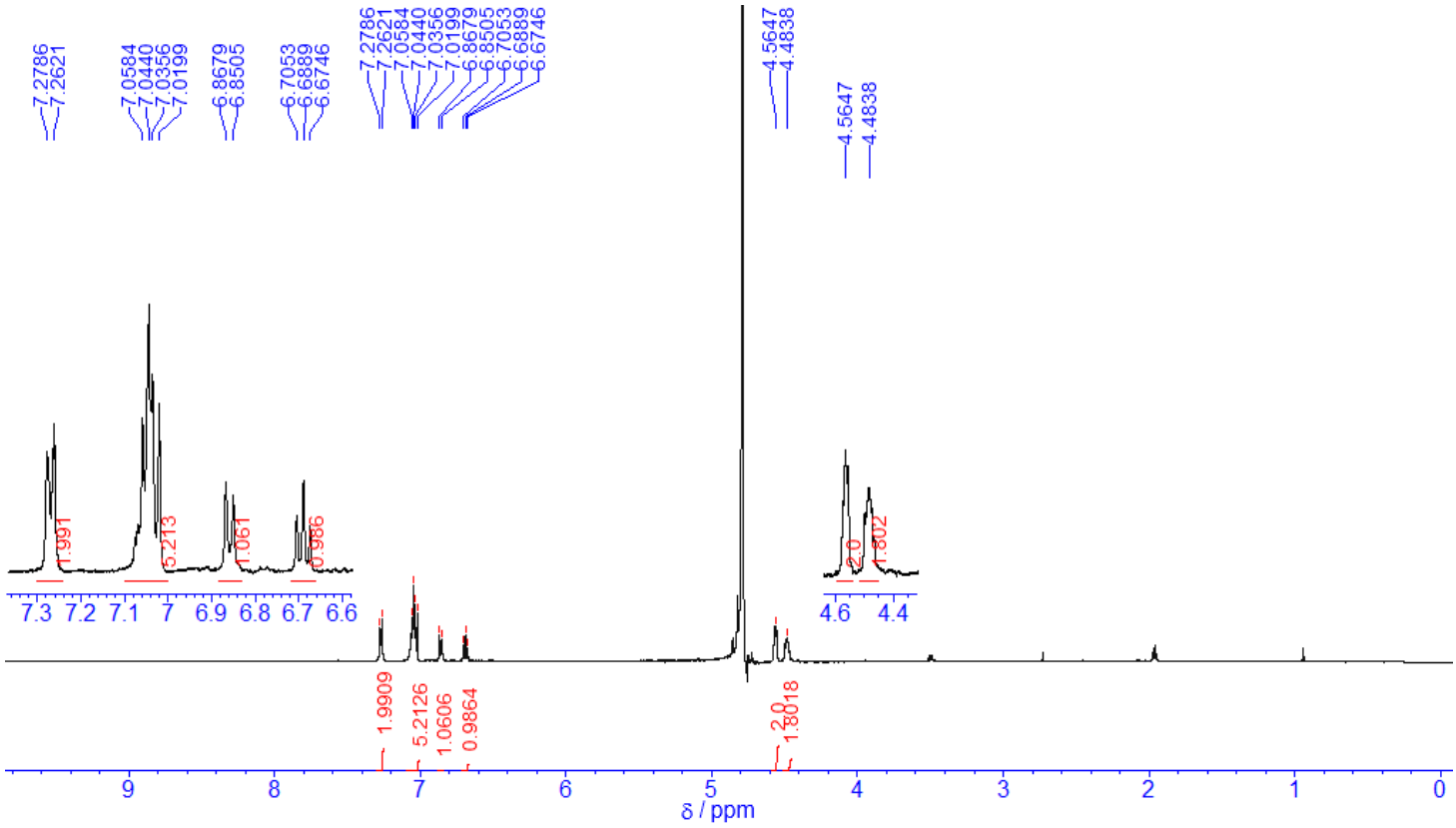

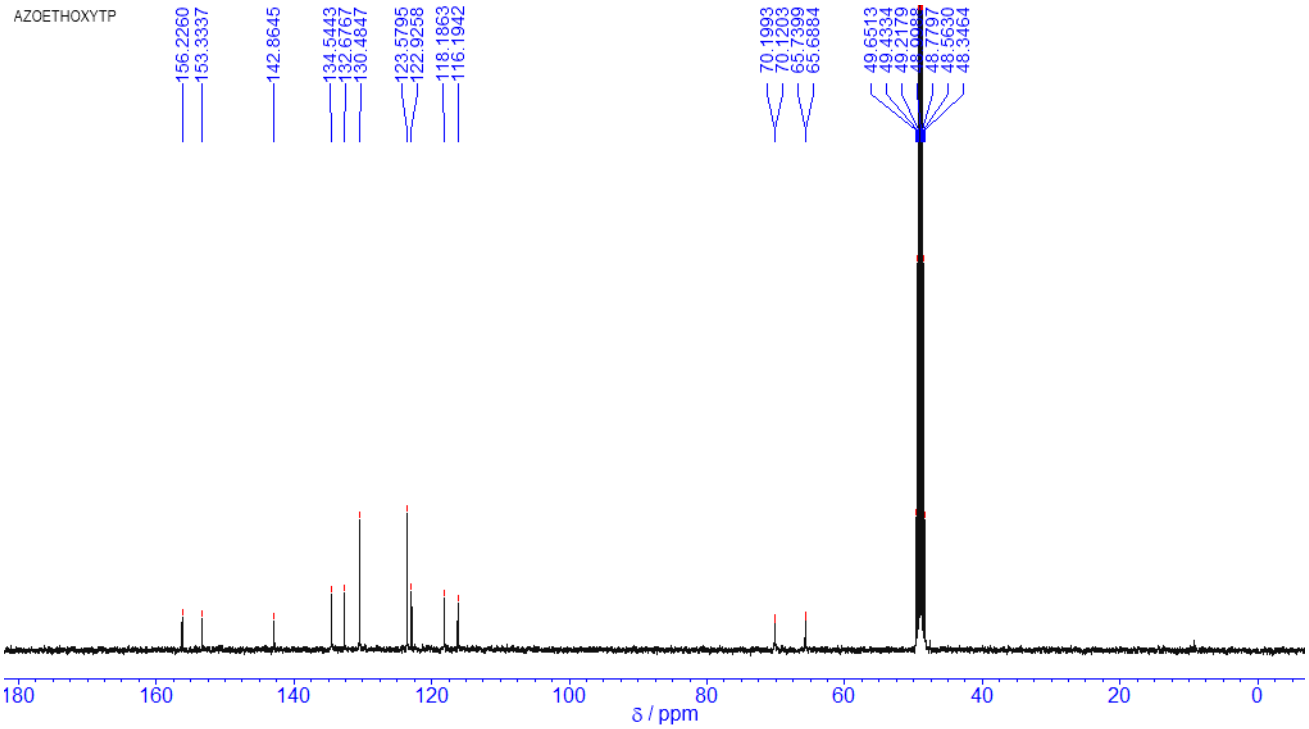

^{1}H NMR and ^{13}C NMR spectra of **1d**

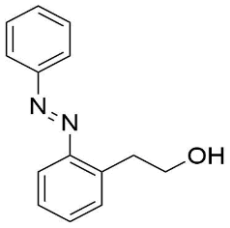

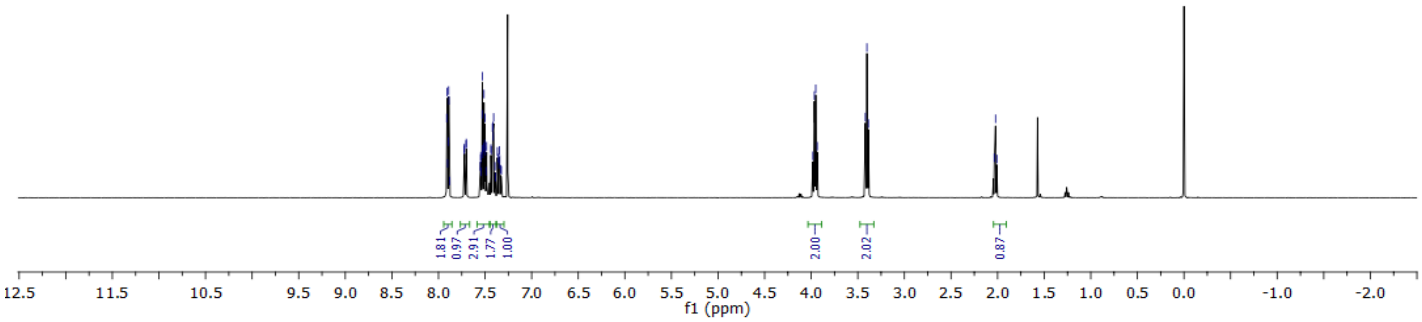

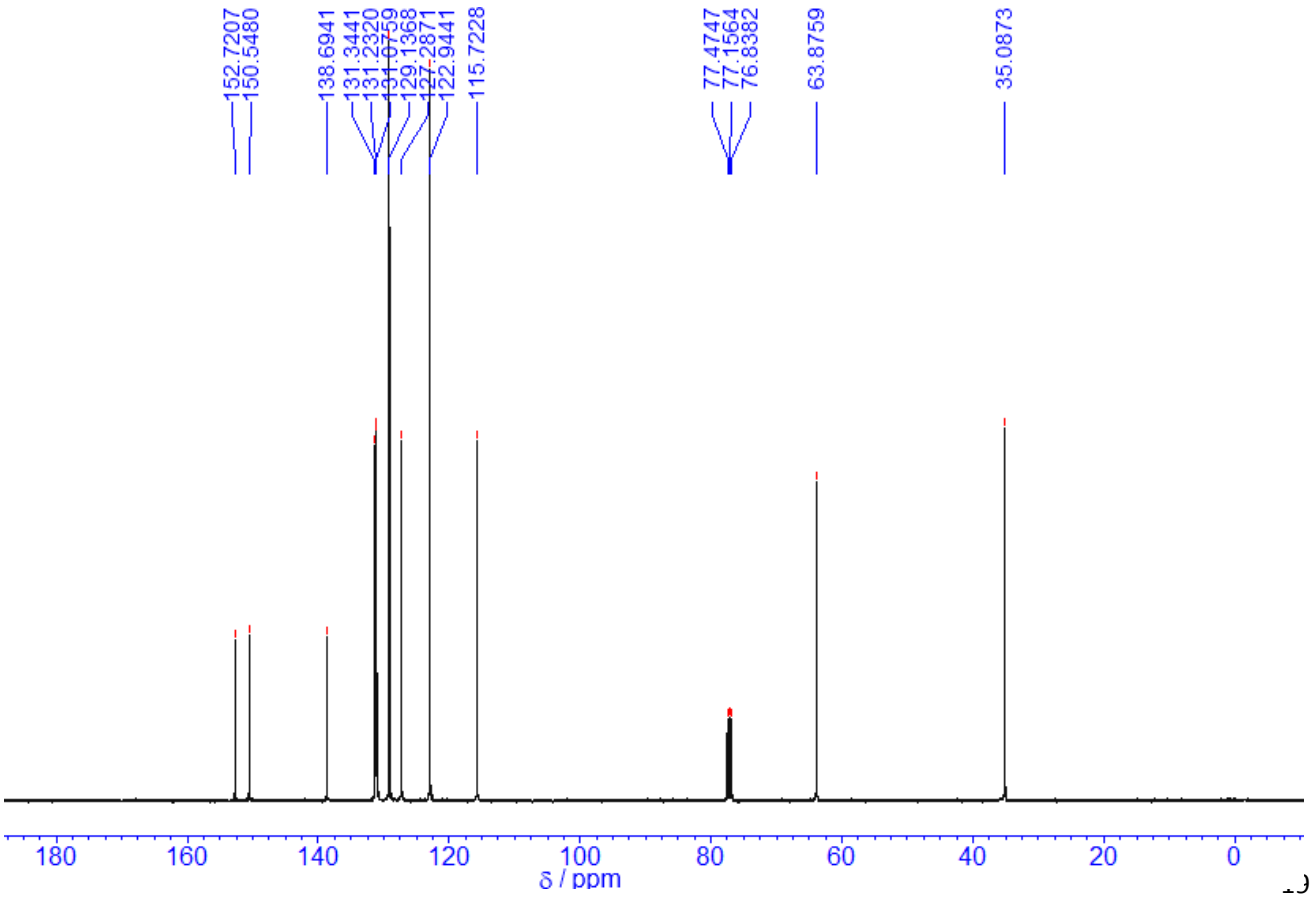

^{1}H NMR and ^{13}C NMR spectra of **2d**

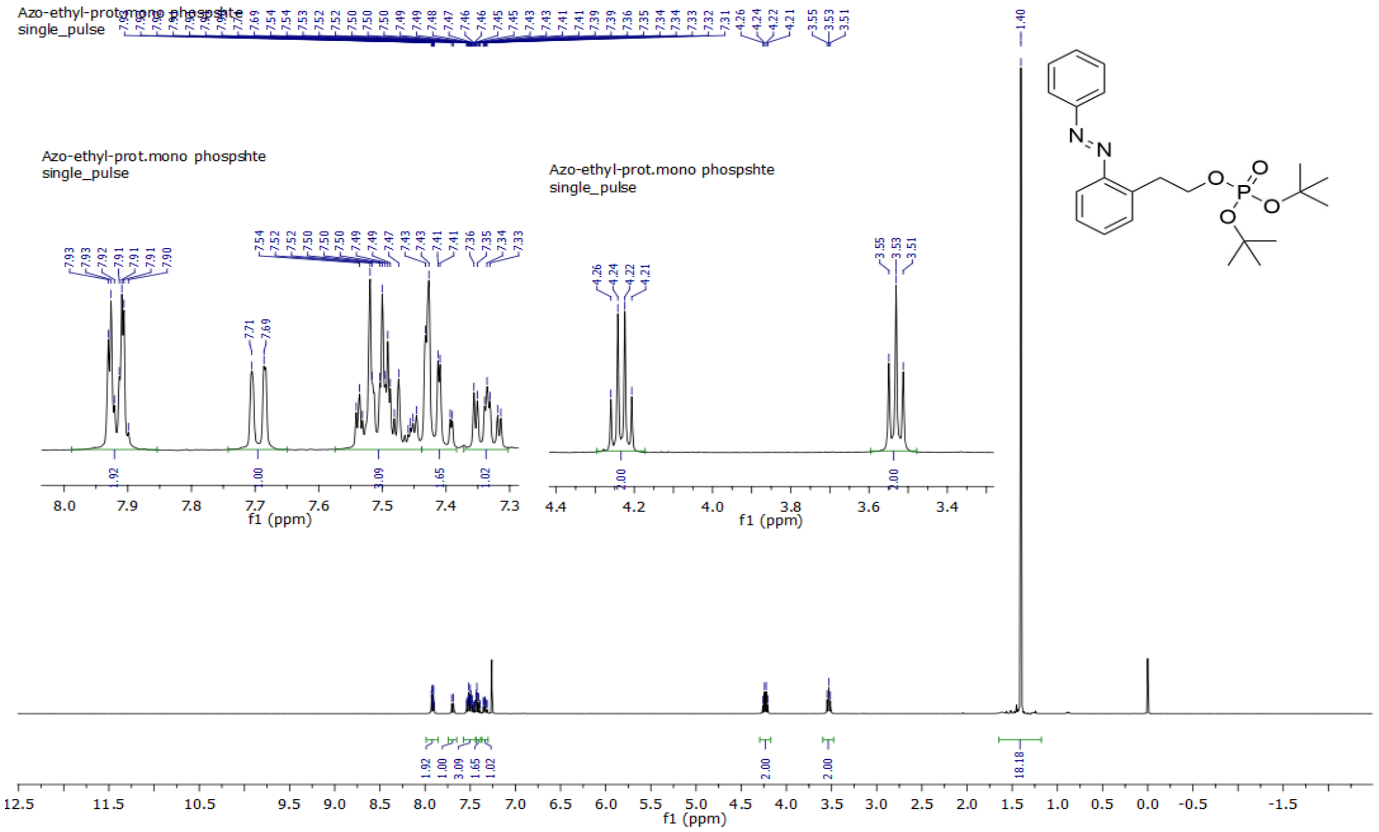

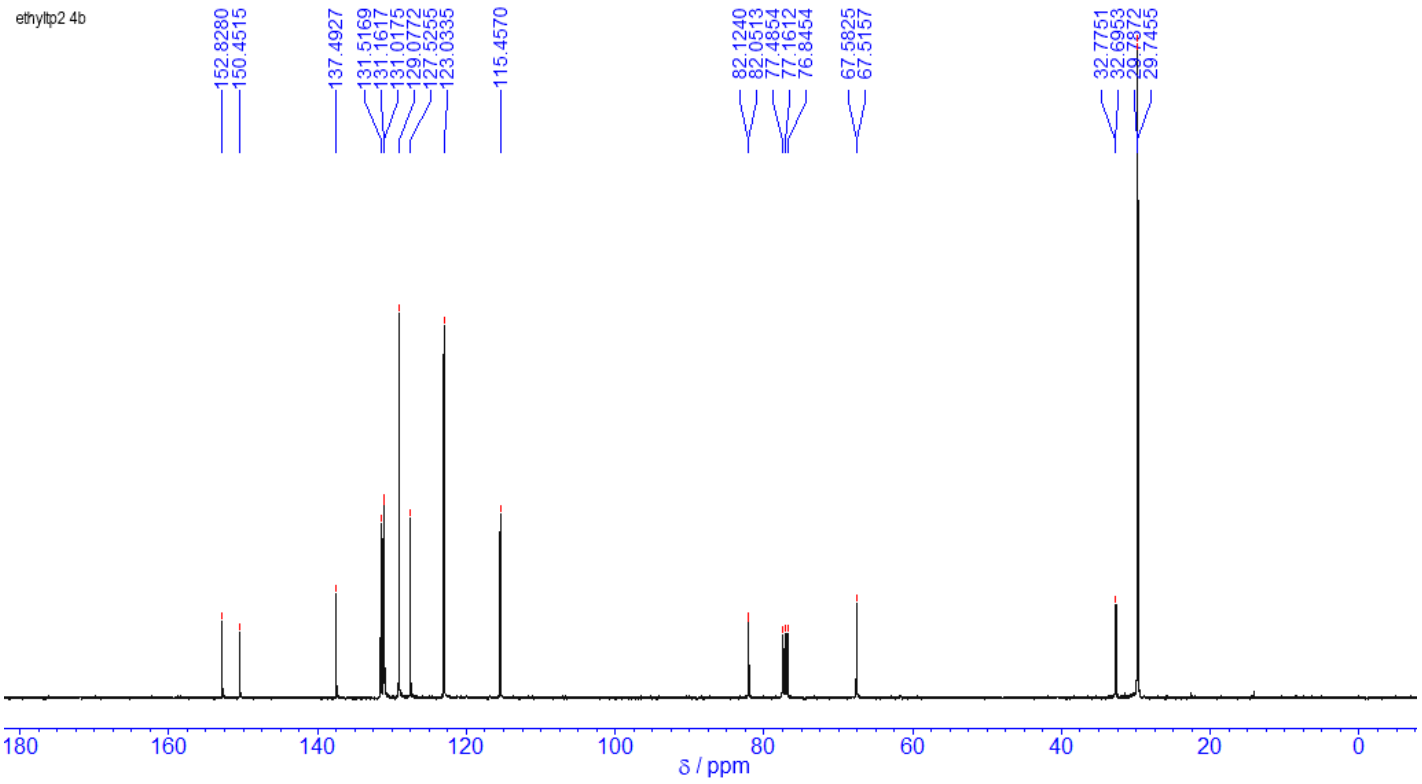

^{1}H NMR and ^{13}C NMR spectra of **3d**

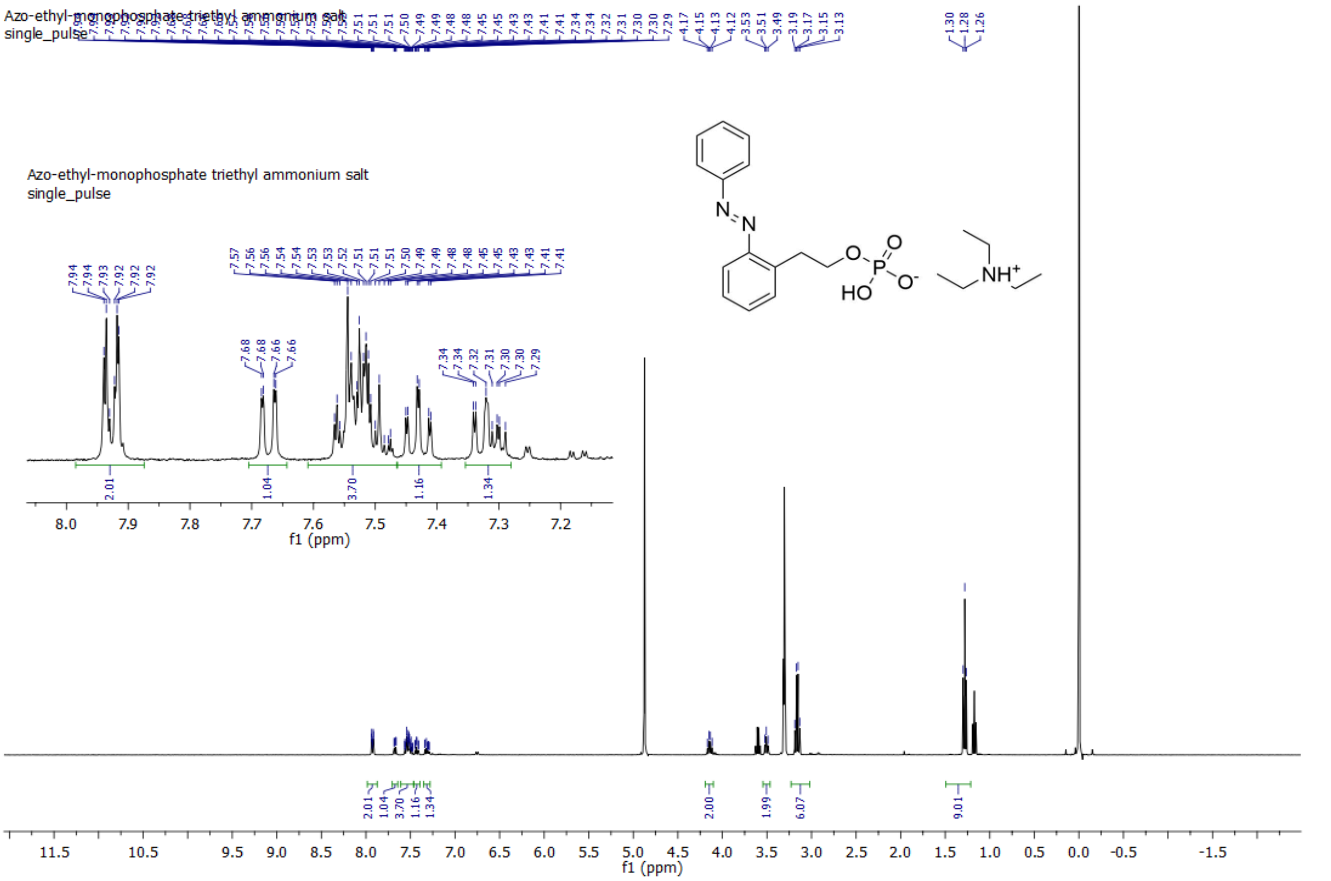

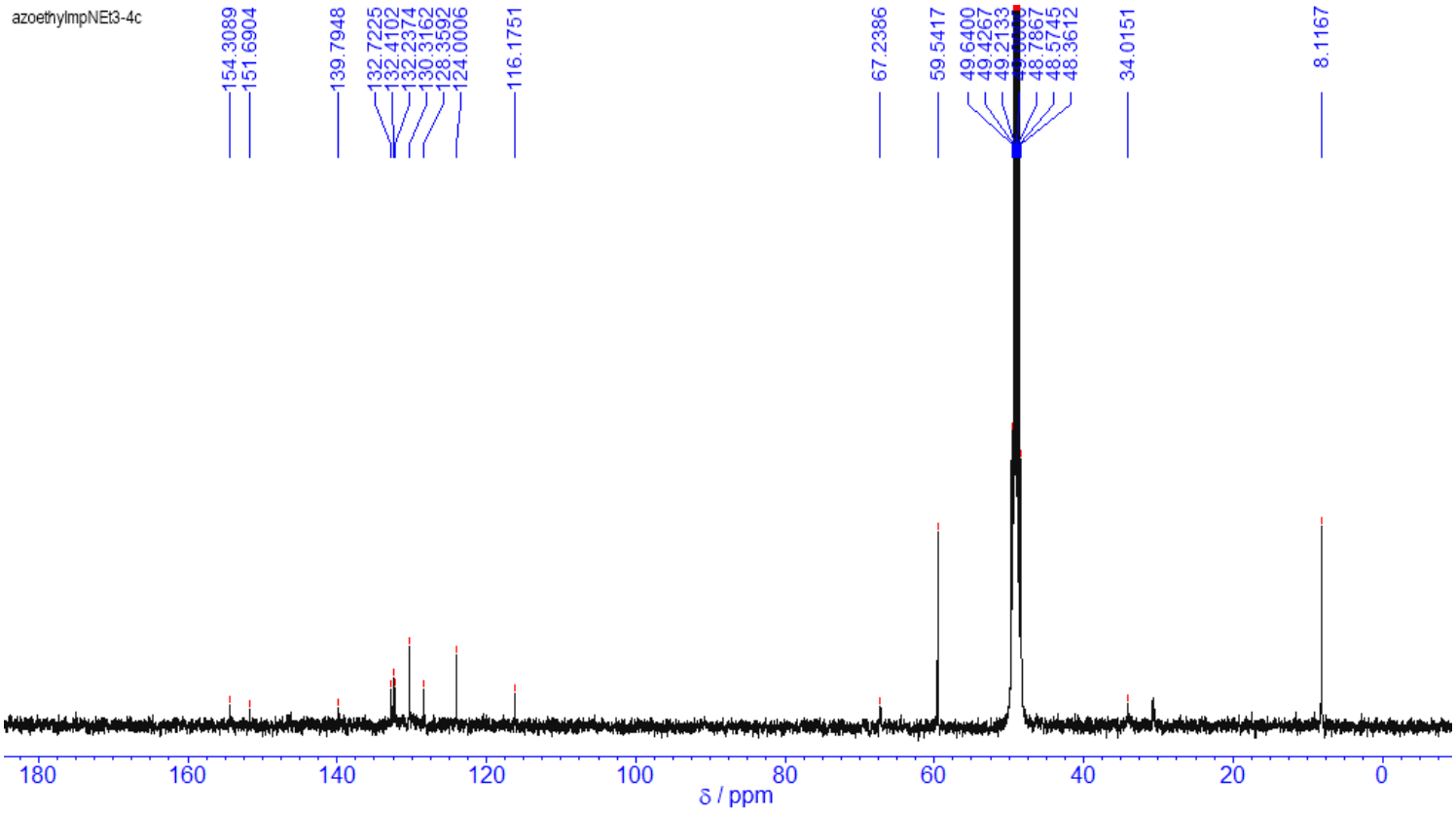

^{1}H NMR and ^{13}C NMR spectra of **4d**

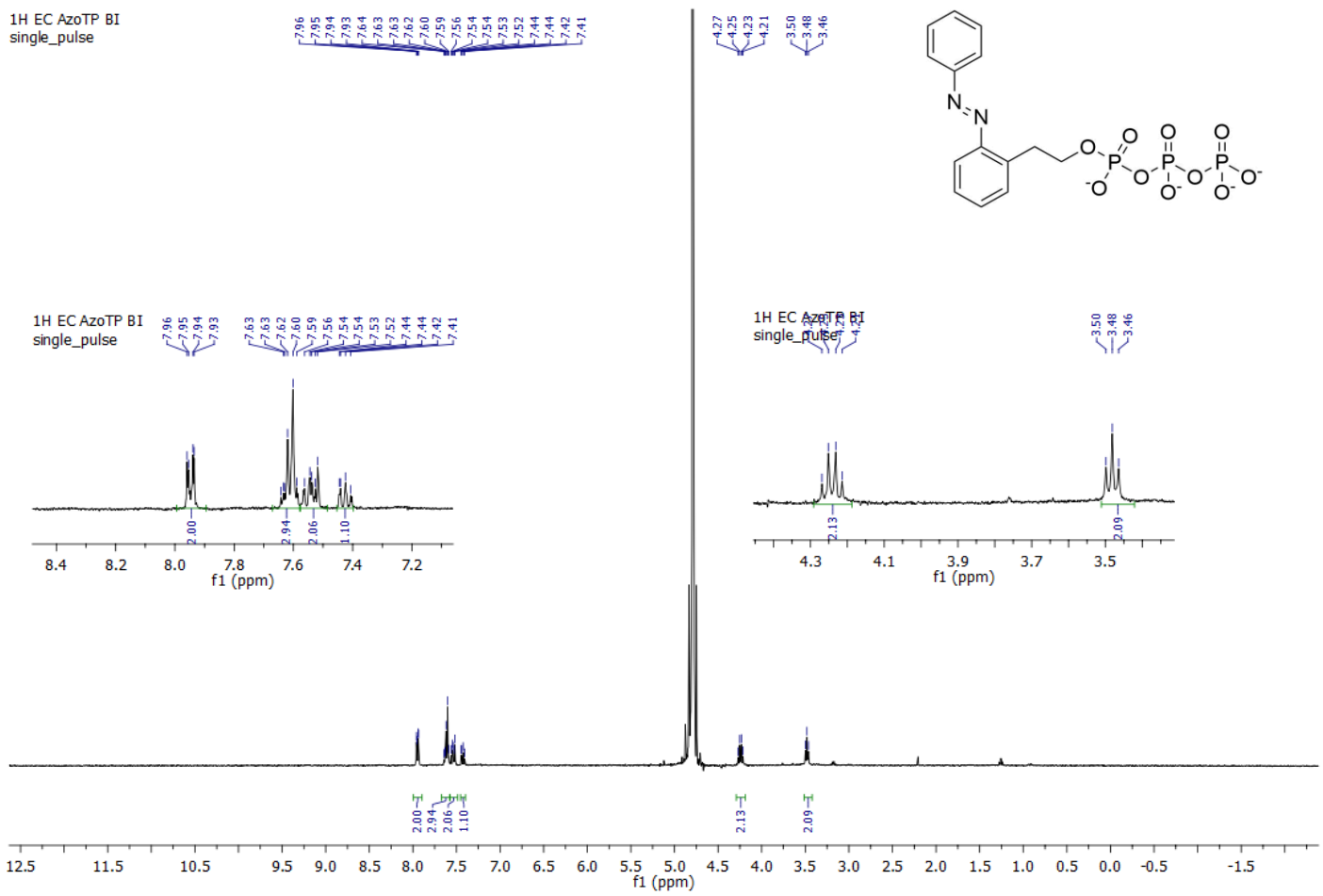

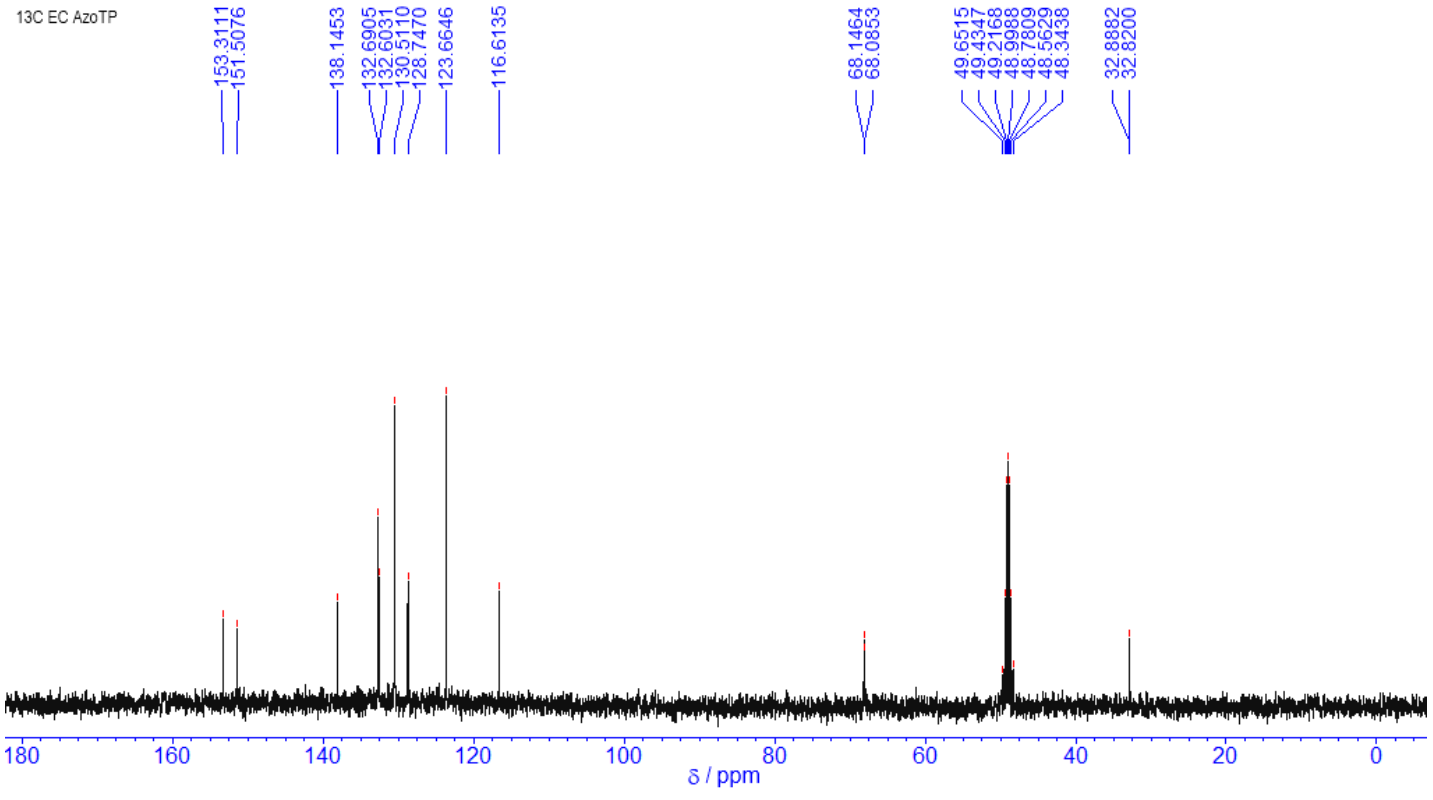

^{1}H NMR and ^{13}C NMR spectra of **5**

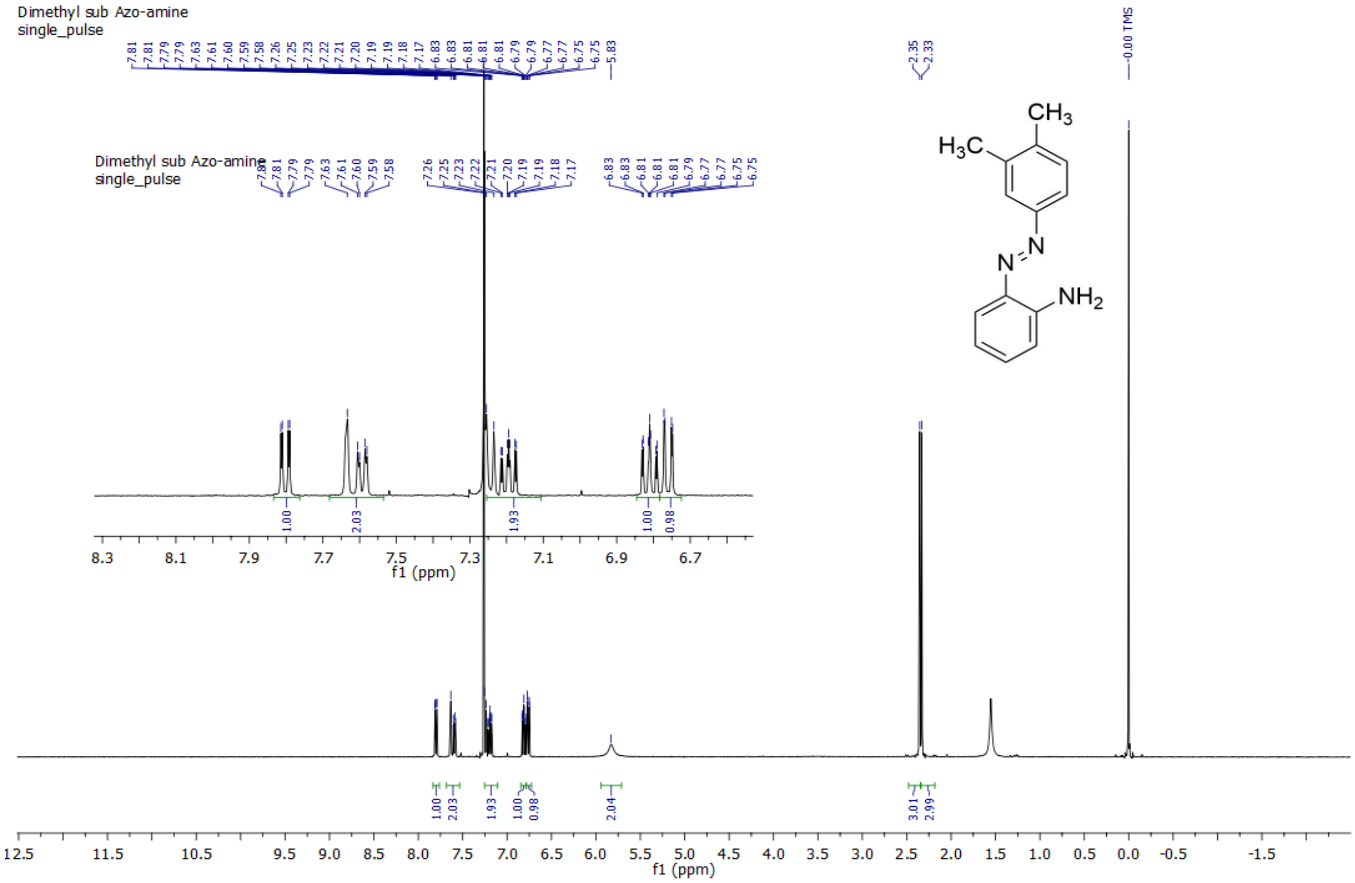

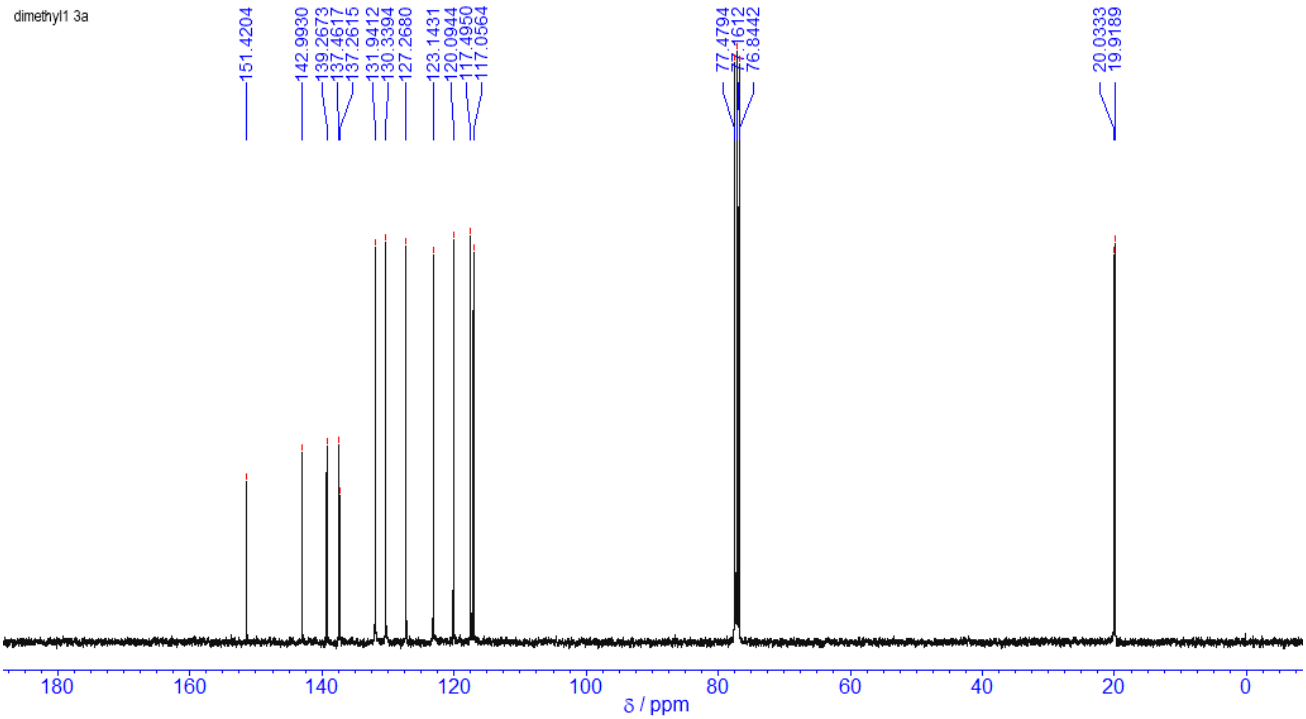

^{1}H NMR and ^{13}C NMR spectra of **6**

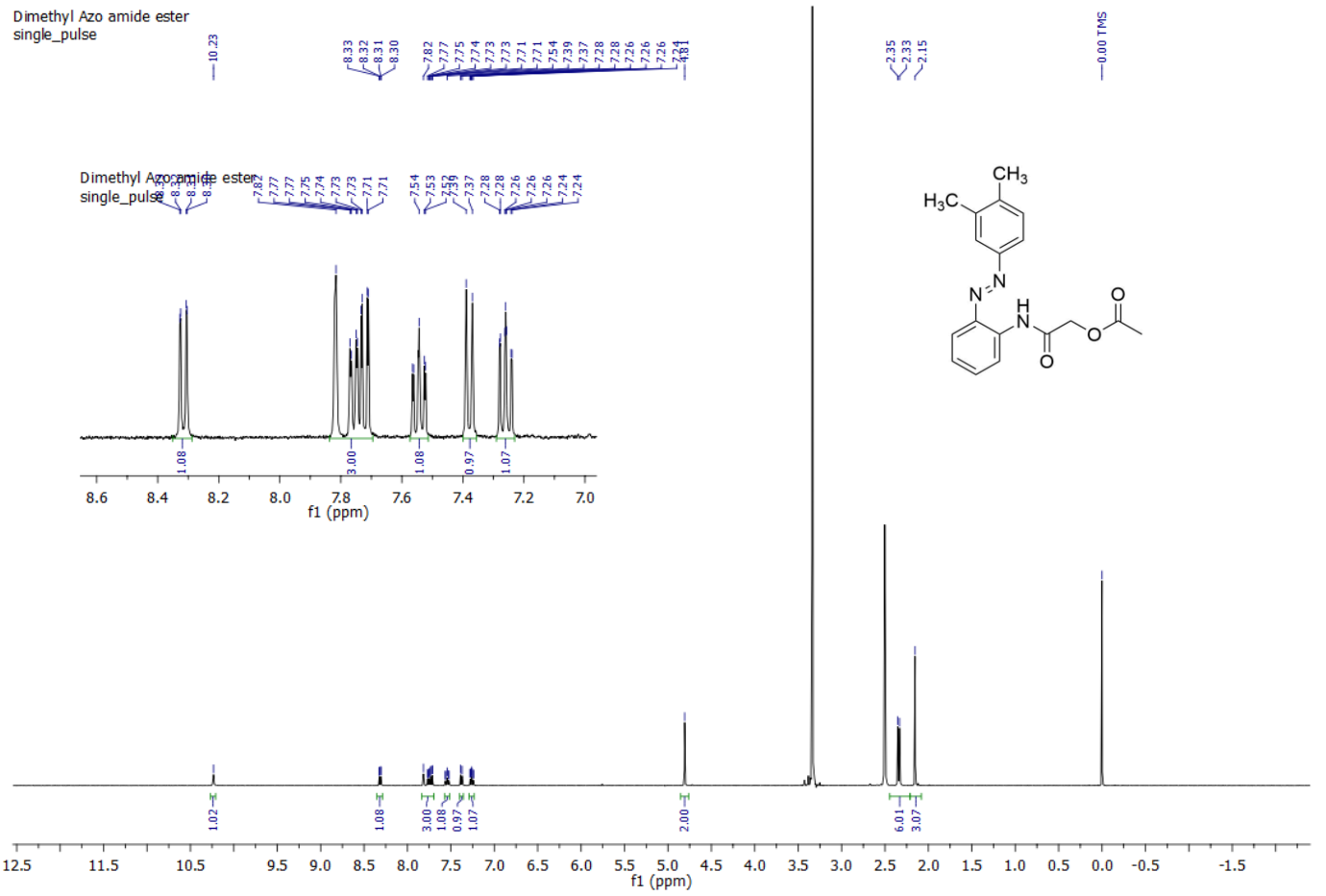

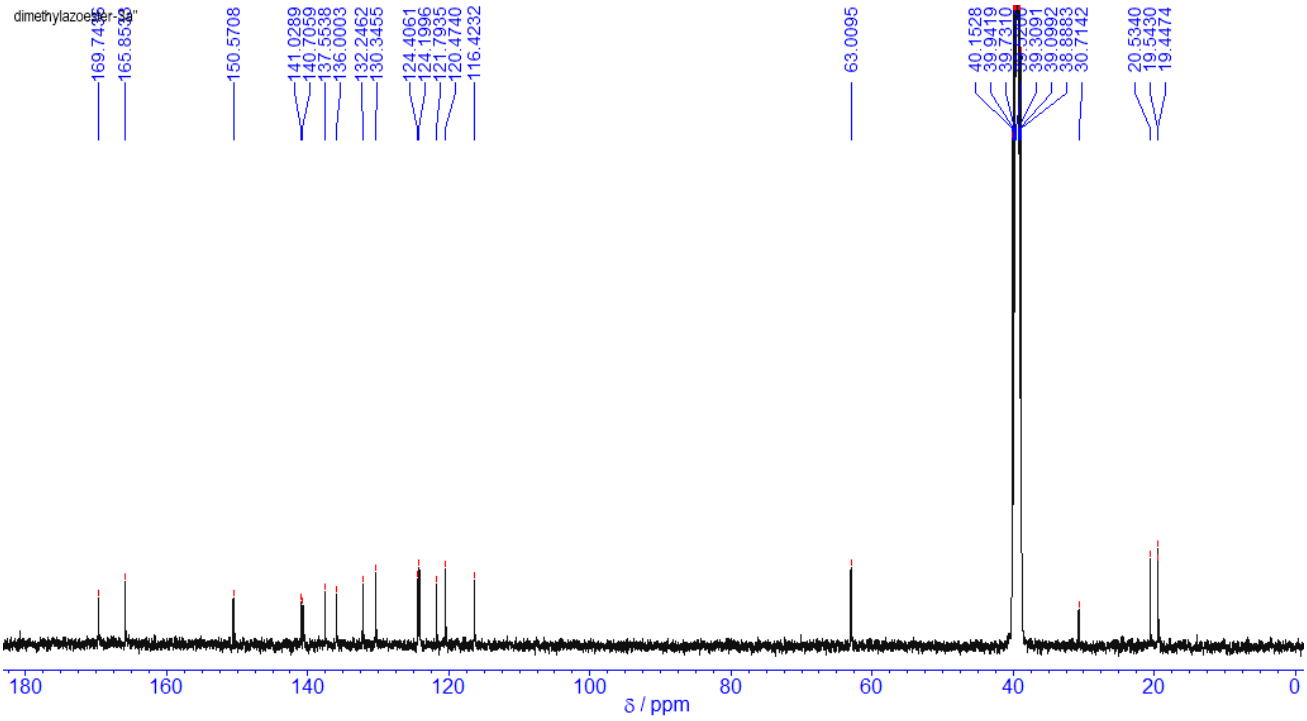

^{1}H NMR and ^{13}C NMR spectra of **1c**

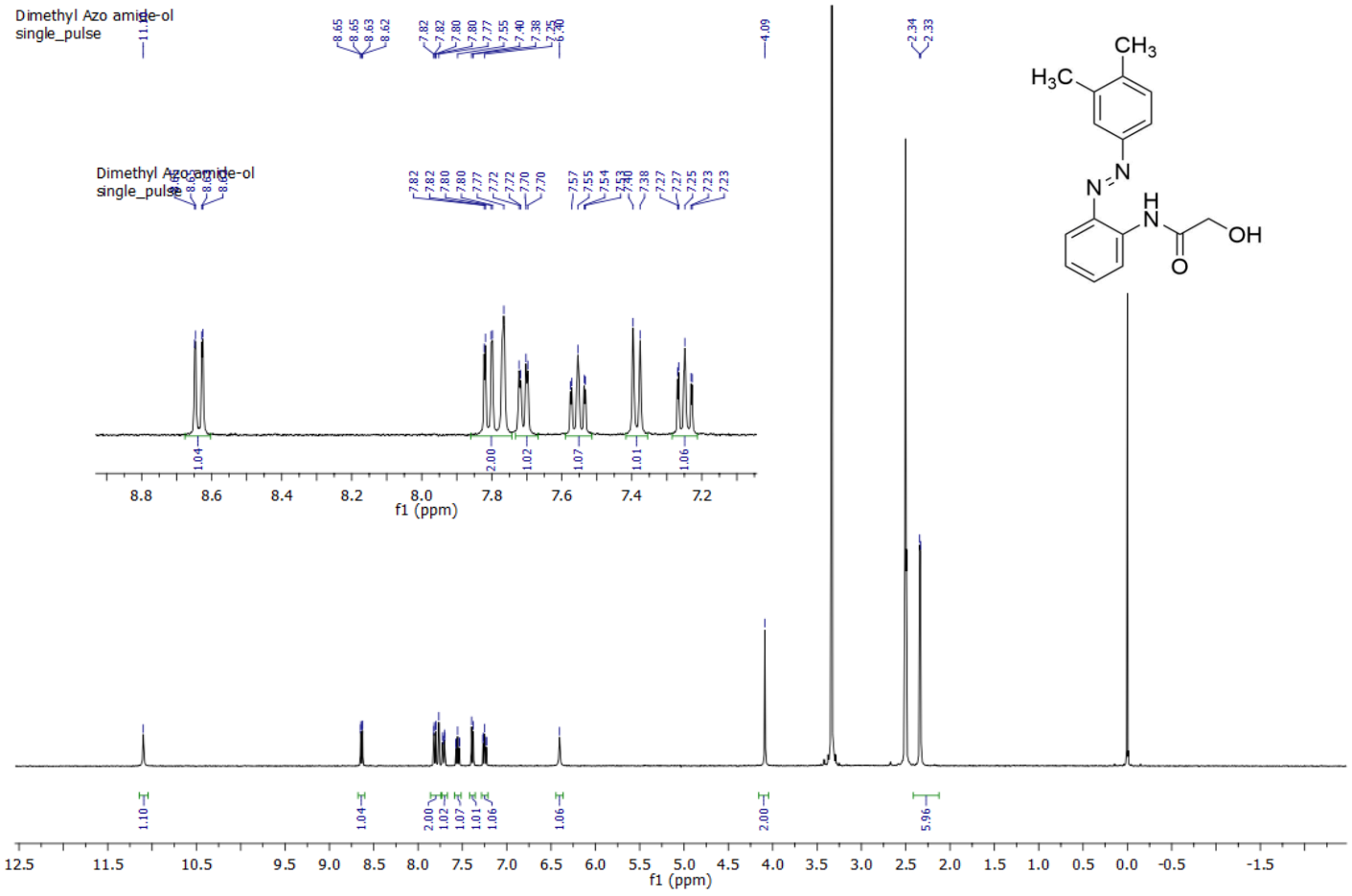

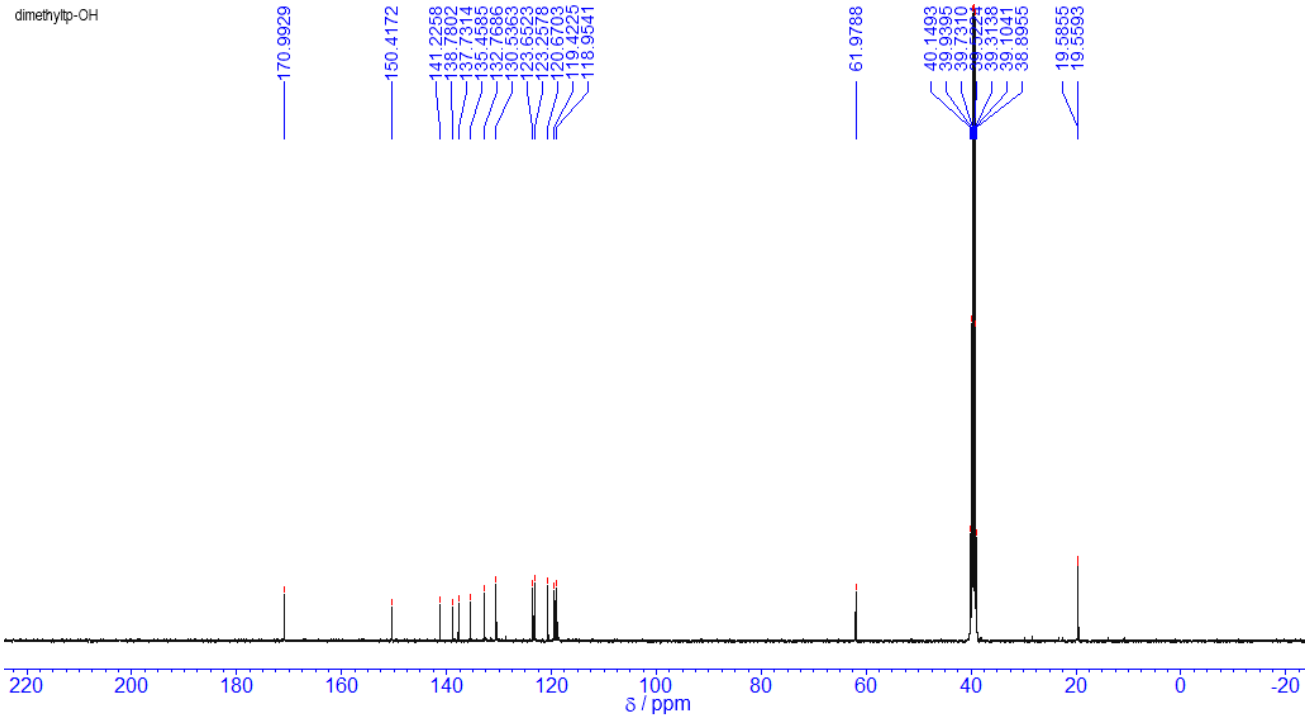

^{1}H NMR and ^{13}C NMR spectra of **2c**

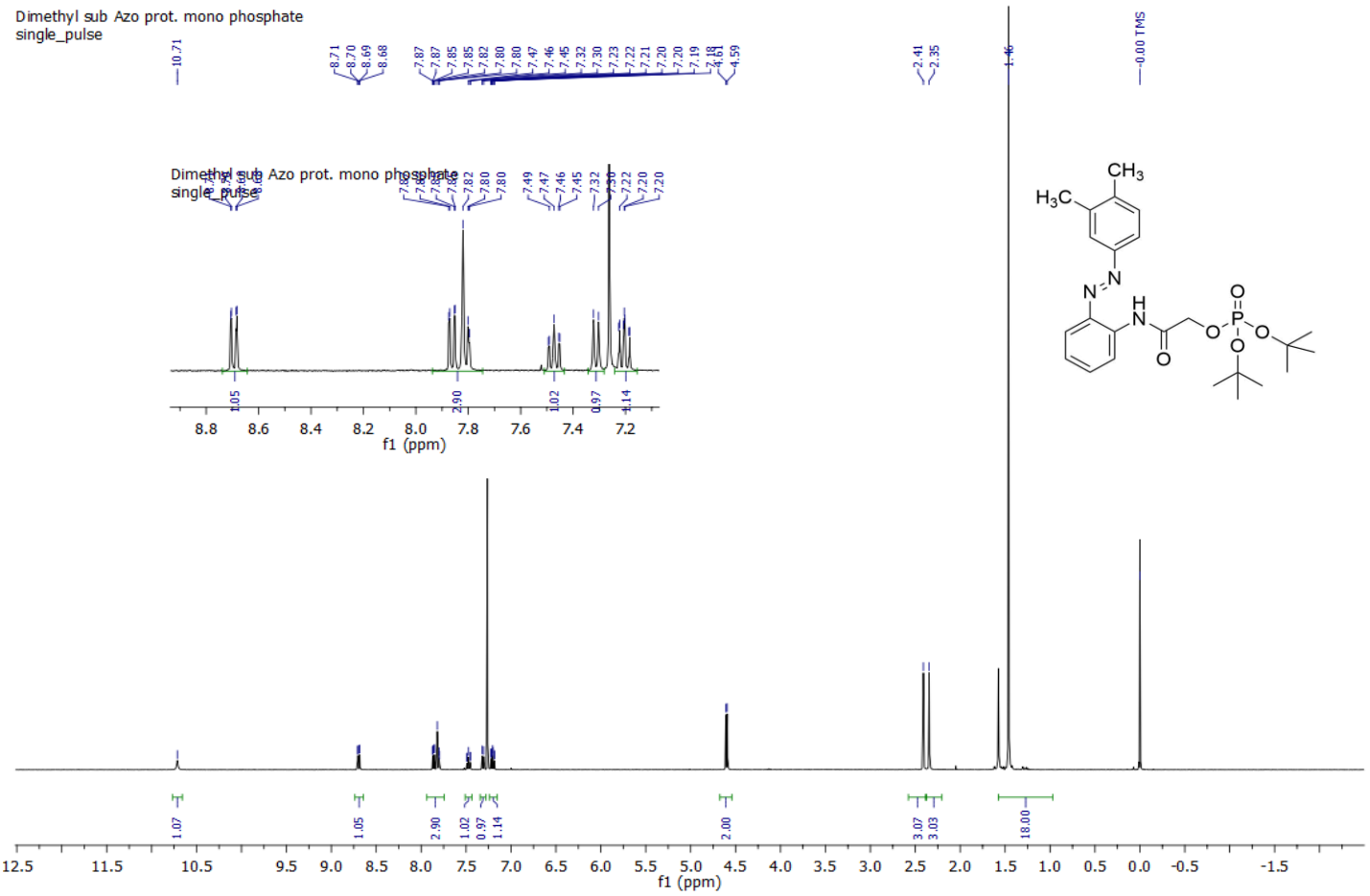

^{1}H NMR and ^{13}C NMR spectra of **4d**

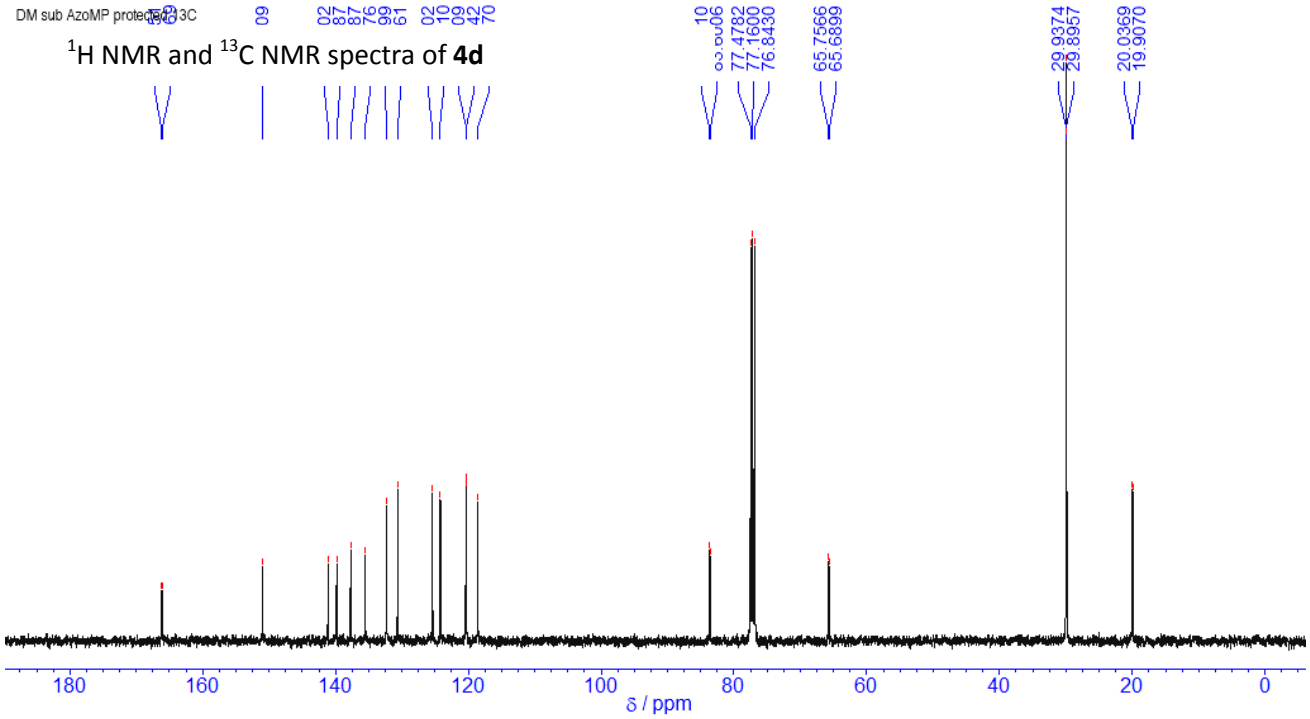

^{1}H NMR and ^{13}C NMR spectra of **3c**

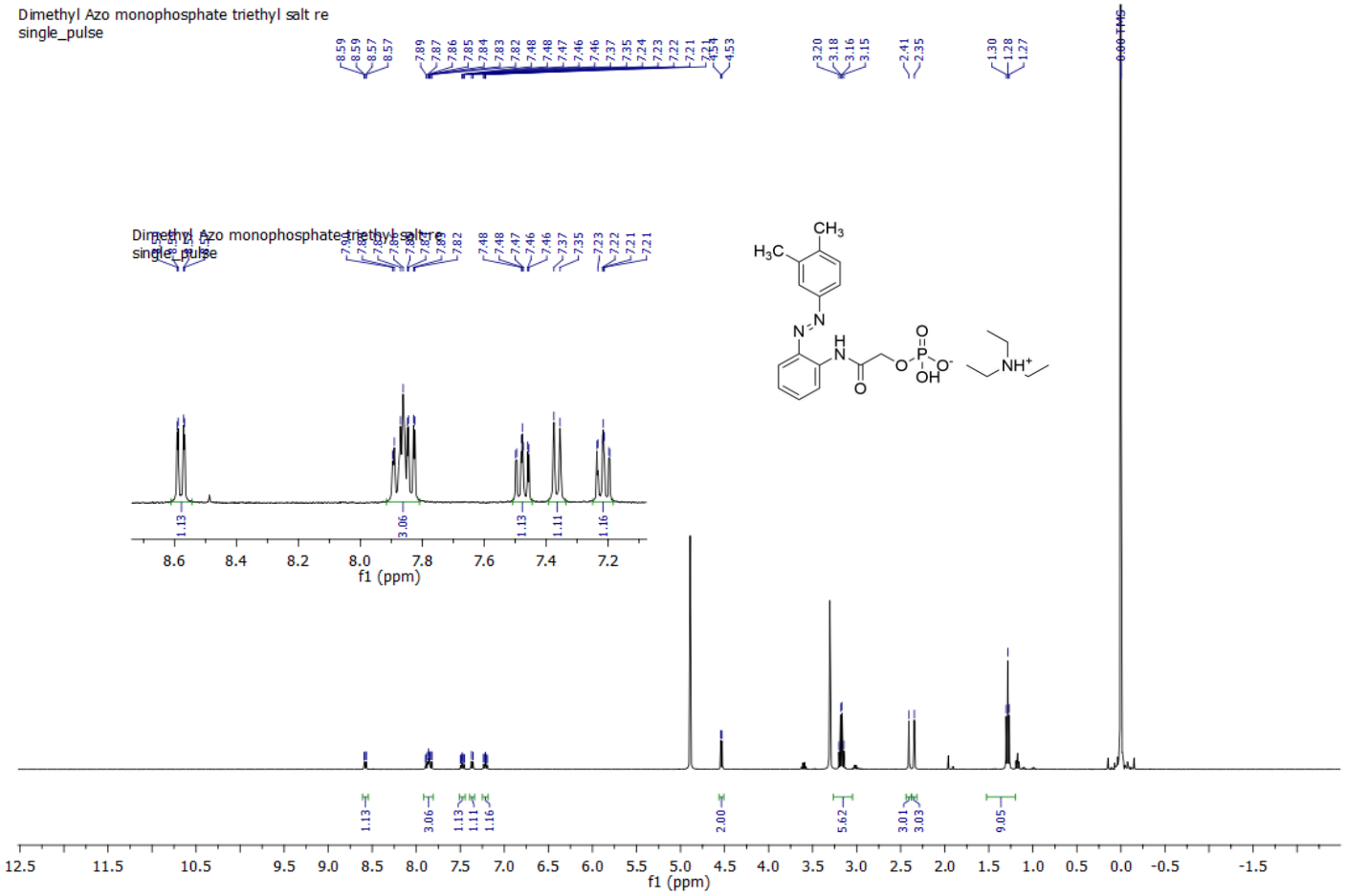

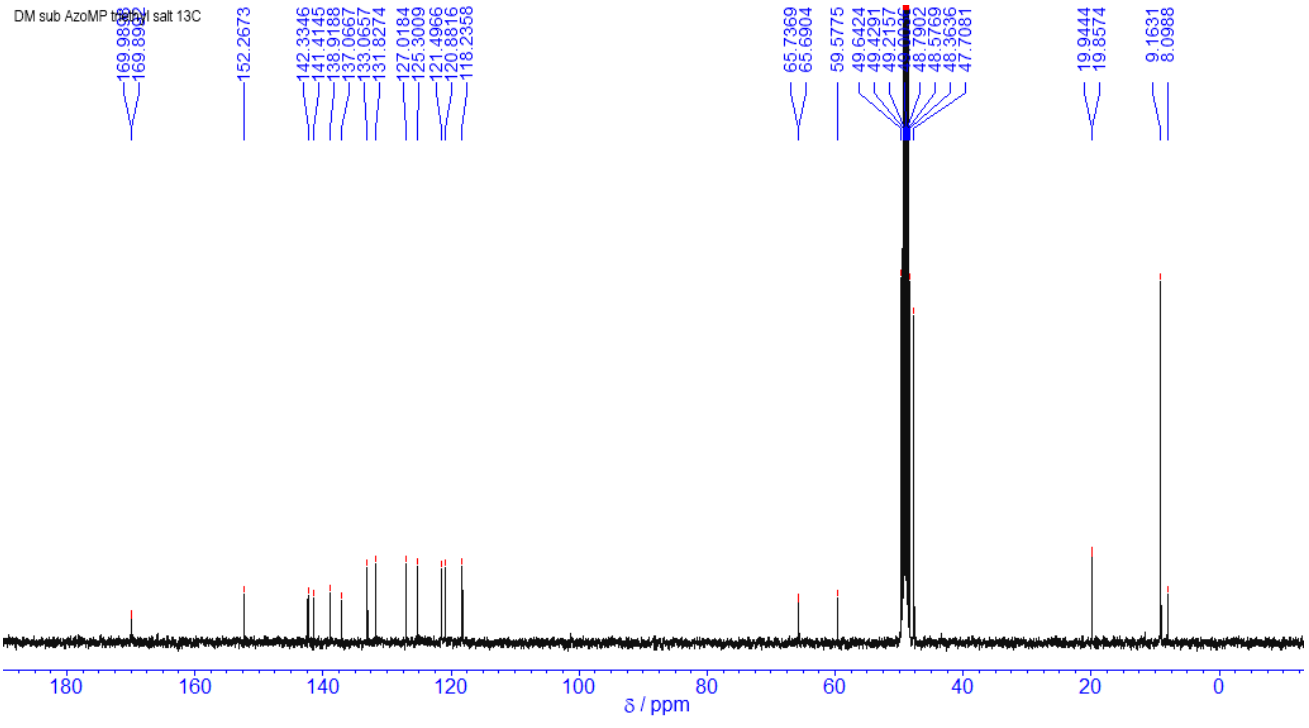

^{1}H NMR and ^{13}C NMR spectra of **3d**

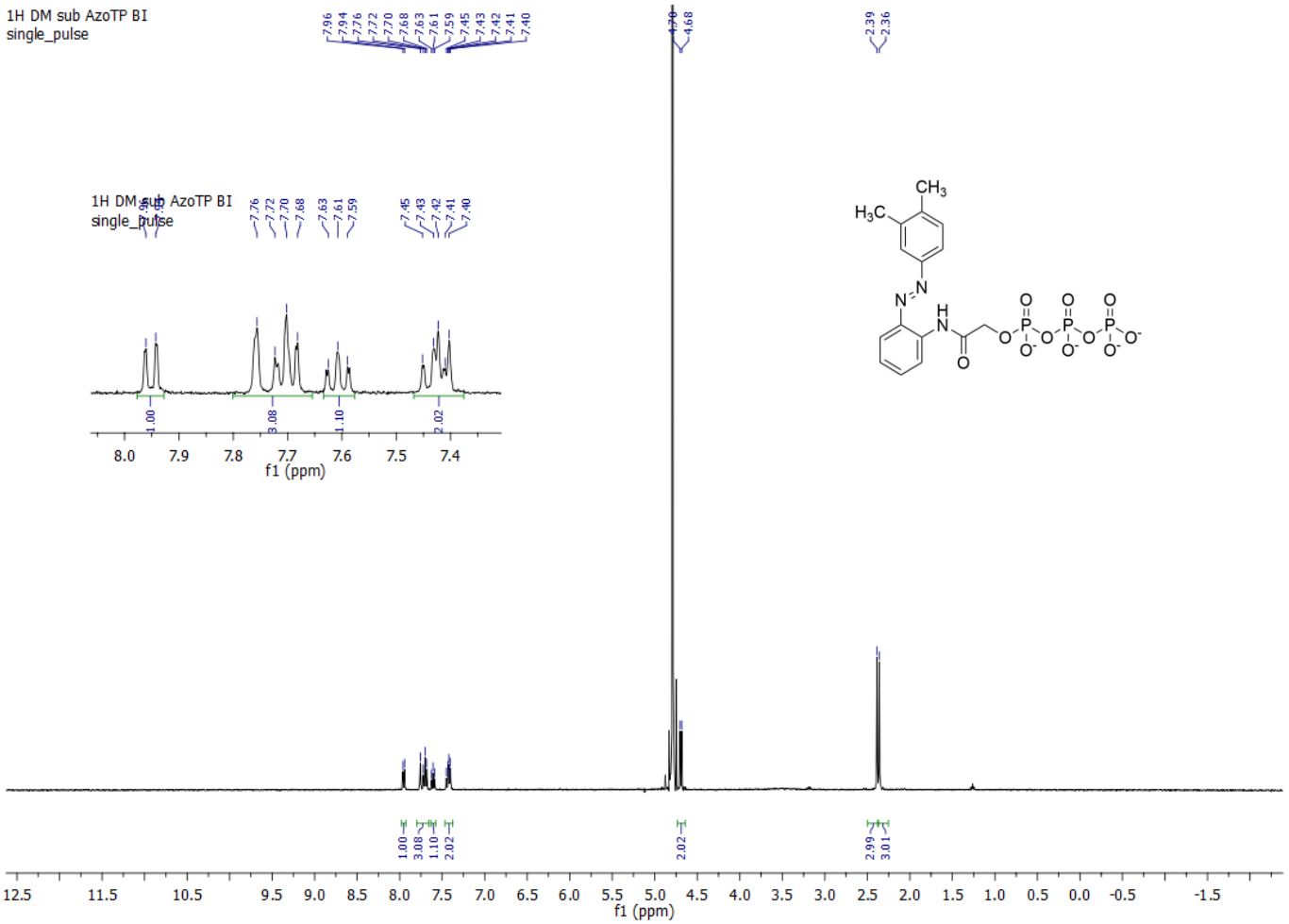

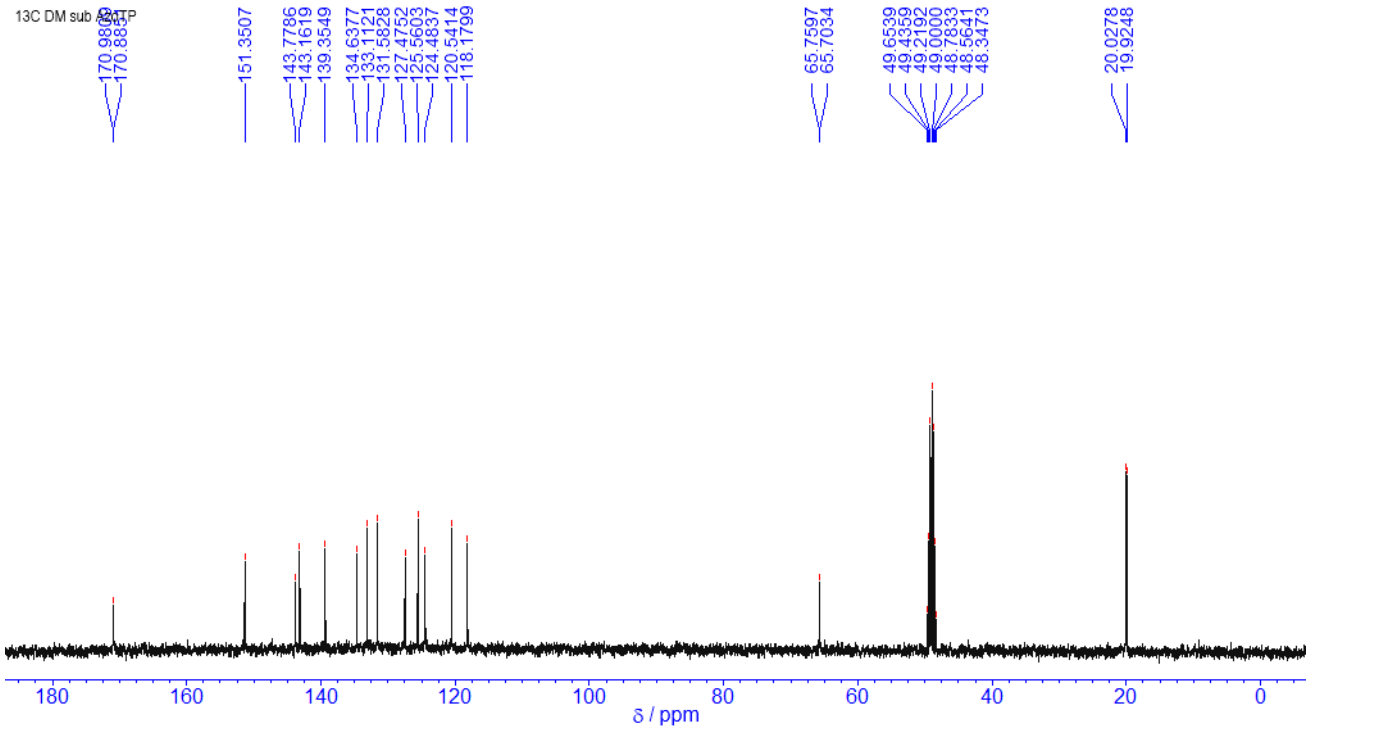

31P NMR spectra of **4c, 4d, 4b.**

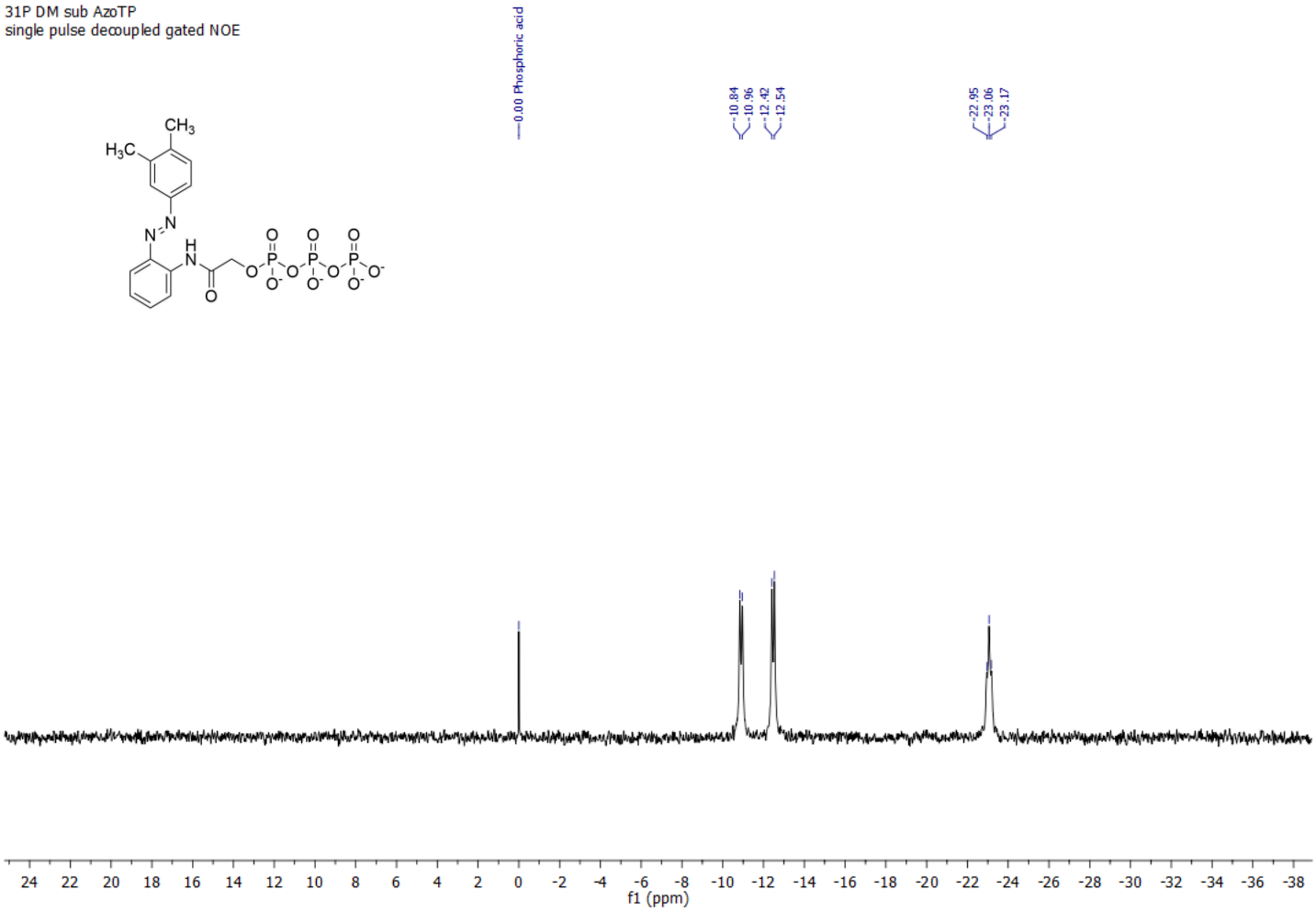

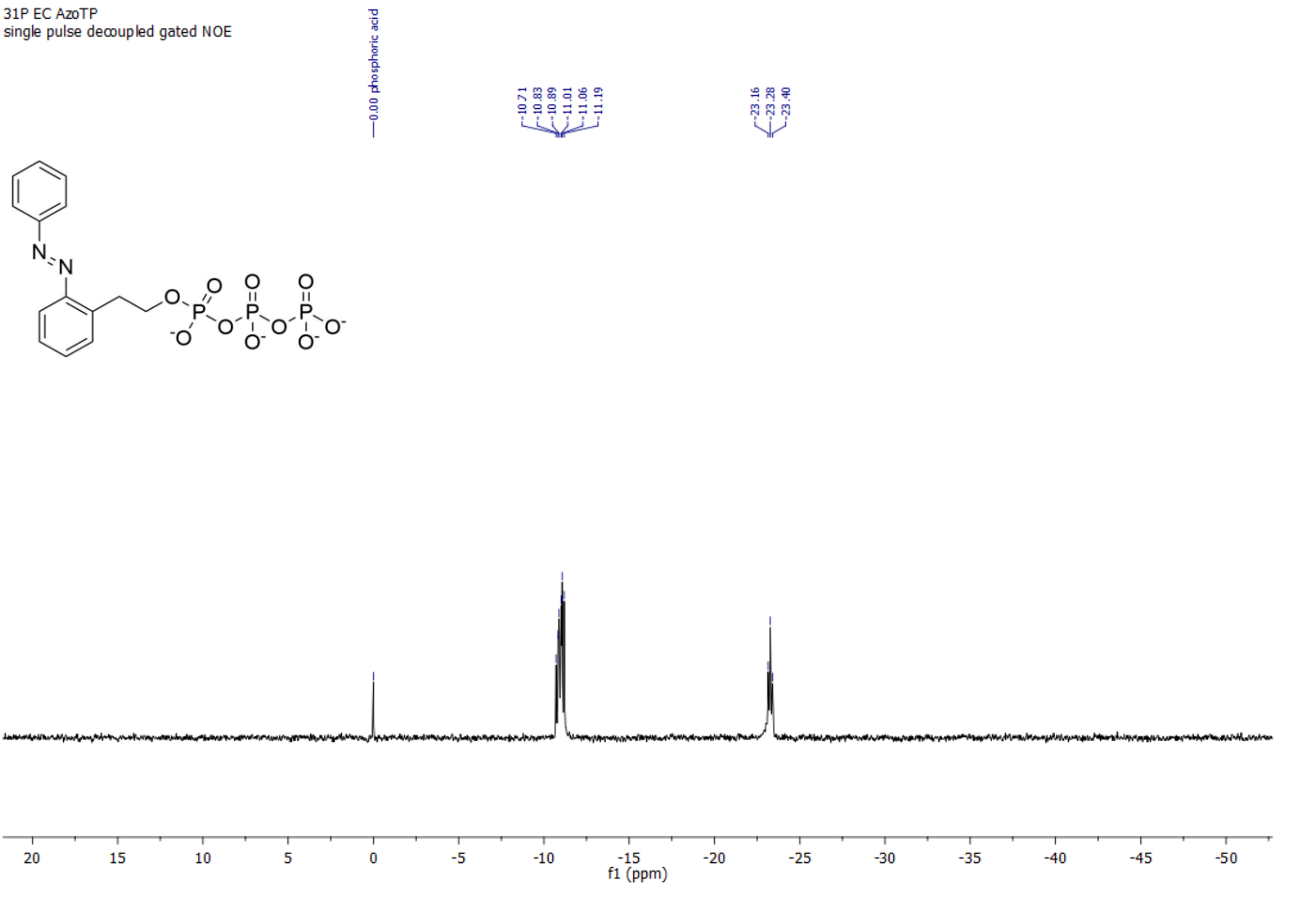

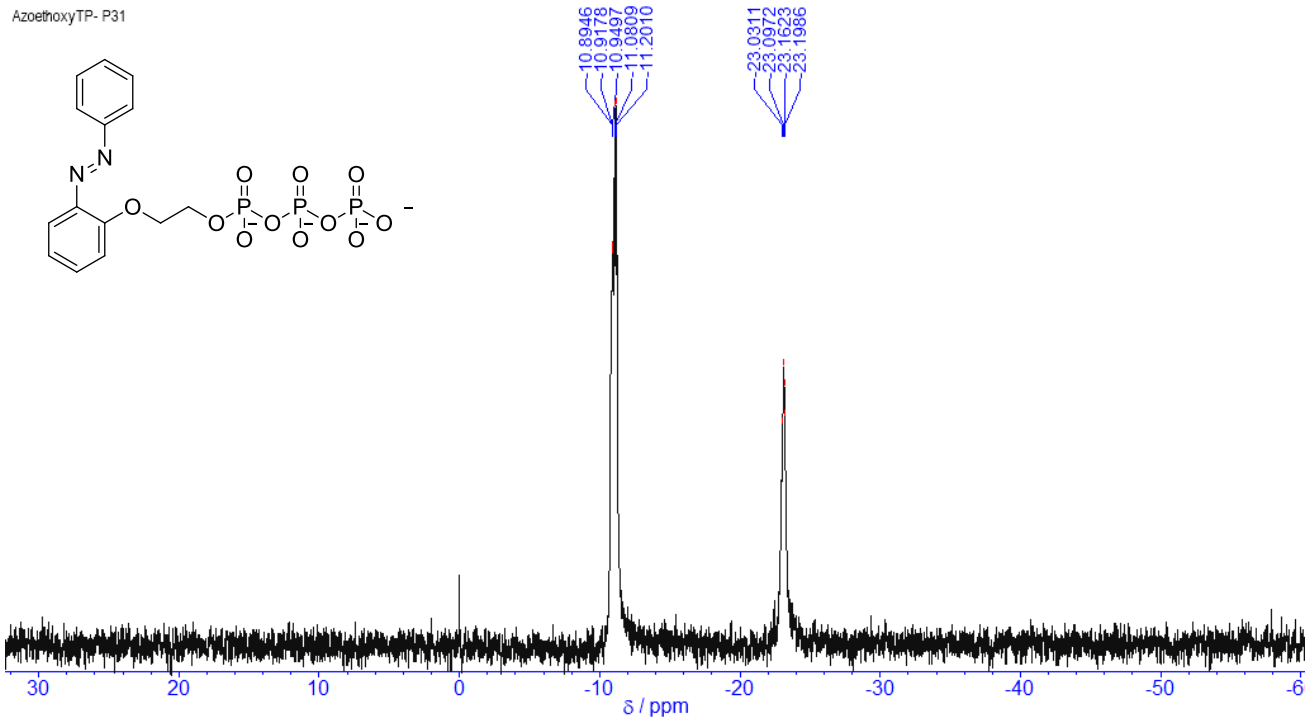
AzoethoxyTP- P31
10.8946
10.9178
10.9497
11.0809
11.2010
23.0311
23.0972
23.1623
23.1986
30
20
10
0
-10
-20
-30
-40
-50
-6
δ / ppm